

NASA TECHNICAL MEMORANDUM

NASA TM-82461

SPACE SHUTTLE STS-1 SRB DAMAGE INVESTIGATION
FINAL REPORT

By Clyde D. Nevins
Structures and Propulsion Laboratory

January 1982

NASA



*George C. Marshall Space Flight Center
Marshall Space Flight Center, Alabama*

(NASA-TM-82461) SPACE SHUTTLE STS-1 SRB
DAMAGE INVESTIGATION (NASA) 53 P
HC A04/MF A01 C SCL 22B

N82-20235

Unclass
G3/16 09300

TECHNICAL REPORT STANDARD TITLE PAGE

| | | | | | |
|---|--|---|---|---|--------------------------|
| 1. REPORT NO. NASA TM-82461 | | 2. GOVERNMENT ACCESSION NO. | | 3. RECIPIENT'S CATALOG NO. | |
| 4. TITLE AND SUBTITLE Space Shuttle STS-1 SRB Damage Investigation Final Report | | | | 5. REPORT DATE January 1982 | |
| | | | | 6. PERFORMING ORGANIZATION CODE | |
| 7. AUTHOR(S) By Clyde D. Nevins | | | | 8. PERFORMING ORGANIZATION REPORT # | |
| 9. PERFORMING ORGANIZATION NAME AND ADDRESS George C. Marshall Space Flight Center Marshall Space Flight Center, Alabama 35812 | | | | 10. WORK UNIT NO. | |
| | | | | 11. CONTRACT OR GRANT NO. | |
| 12. SPONSORING AGENCY NAME AND ADDRESS National Aeronautics and Space Administration Washington, D.C. 20546 | | | | 13. TYPE OF REPORT, & PERIOD COVERED Technical Memorandum | |
| | | | | 14. SPONSORING AGENCY CODE | |
| 15. SUPPLEMENTARY NOTES Prepared by Structures and Propulsion Laboratory, Science and Engineering | | | | | |
| 16. ABSTRACT <p>The physical damage incurred by the Solid Rocket Boosters during reentry on the initial Space Shuttle flight raised the question of whether the hardware, as designed, would yield the low cost per flight desired. An ad hoc committee of technical specialists was chartered to quantify the damage, determine its cause, and recommend specific design changes which would preclude recurrence. Flight data, post-flight analyses, and laboratory hardware examinations were used during the course of the investigation. The resultant findings pointed to two principal causes: (1) failure of the aft skirt thermal curtain at the onset of reentry aerodynamic heating, and (2) overloading of the aft skirt stiffening rings during water impact. Design changes were recommended on both the thermal curtain and the aft skirt structural members to prevent similar damage on future missions.</p> | | | | | |
| 17. KEY WORDS Space Shuttle Design Solid Rocket Boosters Structural Design Thermal Analysis STS-1 Flight | | | 18. DISTRIBUTION STATEMENT Unclassified - Unlimited | | |
| 19. SECURITY CLASSIF. (of this report) Unclassified | | 20. SECURITY CLASSIF. (of this page) Unclassified | | 21. NO. OF PAGES 52 | 22. PRICE NTIS |

TABLE OF CONTENTS

| | Page |
|--------------------------------------|------|
| INTRODUCTION | 1 |
| DAMAGE SUMMARY | 1 |
| A. Aft Skirt Thermal Damage | 2 |
| B. Aft Skirt Structural Damage | 6 |
| C. SRM Structural Damage | 13 |
| FLIGHT DATA | 13 |
| A. Significant Event Times | 16 |
| B. Reentry Thermal Data | 16 |
| C. Water Impact Loads Data | 24 |
| POST FLIGHT ANALYSES | 25 |
| A. Thermal Analyses | 25 |
| B. Structure Analyses | 29 |
| C. Hardware Examinations | 33 |
| FINDINGS | 39 |
| A. Finding 1 | 39 |
| B. Finding 2 | 40 |
| C. Finding 3 | 40 |
| D. Finding 4 | 40 |
| E. Finding 5 | 40 |
| F. Finding 6 | 41 |
| G. Finding 7 | 41 |
| RECOMMENDATIONS | 41 |
| A. Recommendation 1 | 42 |
| B. Recommendation 2 | 42 |
| C. Recommendation 3 | 42 |
| D. Recommendation 4 | 43 |
| E. Recommendation 5 | 43 |
| F. Recommendation 6 | 43 |
| G. Recommendation 7 | 43 |
| H. Recommendation 8 | 44 |
| REFERENCES | 45 |

LIST OF ILLUSTRATIONS

| Figure | Title | Page |
|--------|---|------|
| 1. | A08 aft skirt cable damage..... | 3 |
| 2. | A08 TVC subsystem damage..... | 5 |
| 3. | STS-1 aft skirt damage (A07)..... | 7 |
| 4. | STS-1 aft skirt damage (A08)..... | 8 |
| 5. | Intermediate ring damage..... | 9 |
| 6. | Intermediate ring damage..... | 10 |
| 7. | Thermal curtain remains..... | 11 |
| 8. | Missing thermal curtain retainers..... | 12 |
| 9. | SRM forward stiffener ring (A08)..... | 14 |
| 10. | Aft skirt heating rate (A08)..... | 17 |
| 11. | Internal aft skirt heating rate (A07)..... | 18 |
| 12. | Internal aft skirt heating rate (A08)..... | 18 |
| 13. | Aft skirt skin temperatures (A07)..... | 20 |
| 14. | Aft skirt skin temperatures (A08)..... | 21 |
| 15. | Aft skirt aft ring frame temperatures (A07)..... | 22 |
| 16. | Aft skirt aft ring frame temperatures (A08)..... | 23 |
| 17. | Cavity collapse pressures (A08)..... | 26 |
| 18. | SRM internal pressure (A07)..... | 27 |
| 19. | SRM internal pressure (A08)..... | 27 |
| 20. | SRB water impact loads coordinate system and sign convention..... | 30 |
| 21. | SRB roll orientations at water impact..... | 30 |
| 22. | Cavity collapse peak pressure..... | 31 |
| 23. | Cavity collapse pressure – longitudinal distribution (A08)..... | 31 |

LIST OF ILLUSTRATIONS (Concluded)

| Figure | Title | Page |
|---------------|---|-------------|
| 24 | Aft skirt intermediate ring fracture directions (A07) | 36 |
| 25. | Aft skirt ring measurements | 36 |
| 26. | Aft skirt post and kick ring measurements | 37 |
| 27. | Aft skirt actuator bracket measurements | 37 |
| 28. | Nozzle LSC in relation to thermal curtain retainers | 39 |

ORIGINAL PAGE IS
OF POOR QUALITY

LIST OF TABLES

| Table | Title | Page |
|-------|---|------|
| 1. | A07 TVC Subsystem Damage | 4 |
| 2. | A08 TVC Subsystem Damage | 4 |
| 3. | SRB Measurements Lost During Reentry | 15 |
| 4. | SRB Significant Event Times. | 17 |
| 5. | STS-1 Aft Skirt Structural Temperature Measurements | 19 |
| 6. | Data From Passive Temperature Sensors. | 24 |
| 7. | Nozzle Pyrolysis Gas Composition | 28 |
| 8. | Inflammability Limits With Air. | 28 |
| 9. | Estimated Water Impact Conditions | 29 |
| 10. | Results of Post-Flight Stress Analysis on the Aft Skirt Intermediate Ring | 32 |
| 11. | Aft Skirt Ring Capability at Failure Pressure. | 32 |
| 12. | SRB Attrition Analysis Results | 33 |
| 13. | Tensile Test Results – SRB A07 Aft Skirt Lower Ring Segment | 34 |
| 14. | Tensile Test Results from STS-1 Aft Skirt Intermediate Rings. | 34 |
| 15. | STS-1 Aft Skirt Postflight Dimensional Check Results | 38 |
| 16. | STS-1 Aft Skirt Postflight Versus Preflight Dimensional Comparison. | 38 |

TECHNICAL MEMORANDUM

SPACE SHUTTLE STS-1 SRB DAMAGE INVESTIGATION FINAL REPORT

INTRODUCTION

The successful launch and recovery of two Solid Rocket Boosters (SRB) from the initial Space Shuttle (STS-1) mission provided an early opportunity to evaluate the reuse potential of SRB subsystem hardware. While the design of a SRB subsystem for the ascent portion of the mission is based on conventional (i.e., conservative) design criteria, the design philosophy for SRB reentry and water impact was, rather, to select the most cost-effective design option. This design philosophy entailed accepting varying degrees of risk, from mission-to-mission, that certain components may be damaged, perhaps beyond repair, before the end of their useful life. This philosophy also allowed a "shoot and see" attitude, where significant uncertainty existed, prior to the STS-1 launch, of the expected reentry environment or the capability of a given design approach to survive a predicted environment, and where the development cost for alternate design approaches would have been substantially higher than the selected design. Consequently, the degree of damage found on the recovered STS-1 hardware was of great interest from the standpoints of cost effectiveness of the SRB design and the accuracy of the attrition model used to forecast cost per flight.

Three areas of damage observed on the recovered boosters were identified as being substantially more severe than predicted. These were: (1) structural damage to the aft solid motor case and stiffening rings, (2) general heat damage to components mounted in the interior of the aft skirt, and (3) structural damage to the primary stiffening rings in the aft skirt. An ad hoc committee, composed of engineers representing various disciplines within NASA Marshall Space Flight Center; United Space Boosters, Incorporated, the booster assembly contractor; and Thiokol Corporation, the SRM prime contractor, was formed to investigate these areas of damage. The committee was chartered to accomplish three specific objectives:

- 1) Define the actual damage in specific technical terms.
- 2) Reconstruct the failure scenario based on flight data, postflight analyses, and laboratory tests.
- 3) Recommend specific design changes, if any, which would be cost effective in later launches of SRB hardware.

This report summarizes the evidence gathered and the findings and recommendations generated by the committee. Much additional detail is available in the various letters and reports generated during the course of the investigation.

DAMAGE SUMMARY

The general condition of the STS-1 SRB was well within prelaunch expectations following recovery. A complete external visual examination was performed immediately after the boosters were

removed from the water [1], and a large number of still, color photographs, movie footage, and video tapes were used to document the general appearance of the basic structure and subsystem hardware.

The initial inspection revealed three general areas where damage was significantly greater than expected. It was most apparent that the interior of the aft skirts on each SRB had been exposed to high heating resulting in thermal damage to TVC subsystem components and electrical wiring. Further, the stiffening rings in the interior structure of the aft skirt were damaged; in particular, the intermediate ring of the three stiffening rings was severely damaged on both recovered boosters. Finally, the aft motor case segments were found to have significant damage to the bolt-on stiffening rings, and one segment on the left-hand booster (A07) had a visible flattened area ("oil can") in the case wall.

Following the formation of the ad hoc committee, these damaged areas were carefully inspected and the damage was defined in detail down to the component level. In the paragraphs below, the results of the detail inspections are summarized for each of the three areas investigated.

A. Aft Skirt Thermal Damage

The subsystem hardware within the aft skirt, consisting of the thrust vector control (TVC) hardware, electrical cables, and instrumentation sensors (and their associated wiring), were inspected in detail in both the left-hand (A07) booster and the right-hand (A08) booster following the return of the hardware to MSFC. In general, the components in A08 incurred substantially more fire damage than did those in A07.

1. Cable Damage. A general inspection of electrical cabling was performed before removal [2,3], and a series of photographs were taken to record the damage. Figure 1 shows one such photograph taken of the A08 cabling prior to removal. In general, all cabling below the forwardmost ring showed some thermal damage, while cables routed above this ring were undamaged. Both A07 and A08 booster cabling suffered substantial thermal damage with those in A08 being the more severely damaged.

a. A07 Cables. Cables below the intermediate stiffening ring were the more severely damaged, with moderate damage up to the upper ring, and little or no damage to those cables above the upper ring. Although some cables were parted, none were burned in two, but appeared to have been mechanically broken, perhaps by aerodynamic buffeting. The breaks occurred at various locations, some just behind the connectors. All of the water-tight jackets on reusable cables showed evidence of leakage with corrosion at the interfaces with the water-tight connectors.

b. A08 Cables. Cables in the right-hand booster suffered substantially more damage than those in the left-hand booster, although the damage was of the same type as seen on A07. The presence of a heavy coating of smoke residue on all interior surfaces made visual determination of fire damage difficult.

2. TVC Damage. There was a substantial difference in TVC damage between the LH (A07) booster and the RH (A08) booster [4]. The dual auxiliary power units and hydraulic power supplies ("tilt" and "rock") of A07 sustained mostly cosmetic damage, whereas the comparable A08 hardware was much more severely damaged. The greater A08 damage appeared to be the result of being exposed to either higher heating or a fire within the aft skirt cavity.

ORIGINAL PAGE
BLACK AND WHITE PHOTOGRAPH

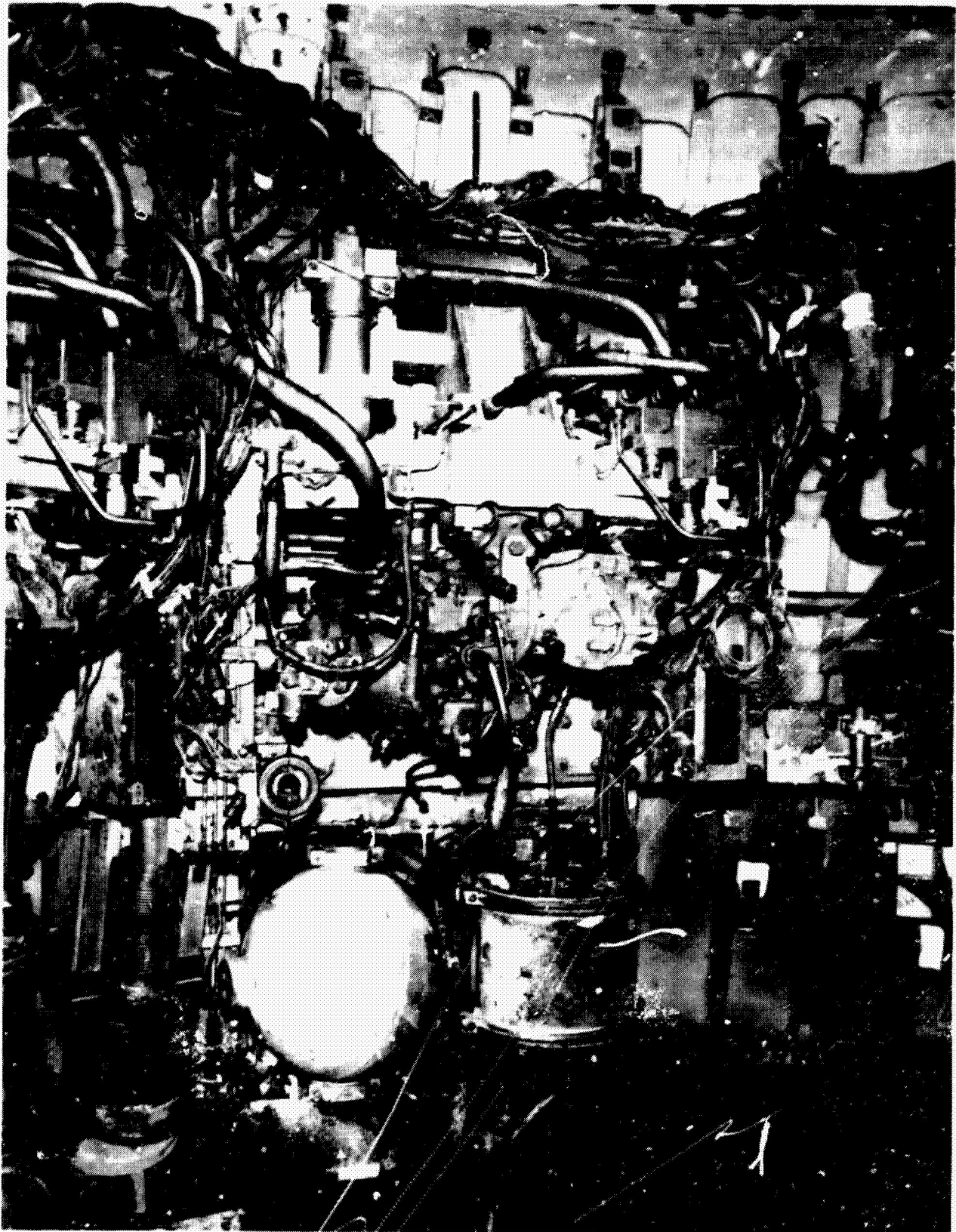


Figure 1. A08 aft skirt cable damage.

The A07 hydrazine and hydraulic oil containing elements were still sealed, and no loss of fluids had occurred. Both the left (rock) and right (tilt) components were judged, from external examination, to be worthy of refurbishment. Some minor water impact damage was noted and this is shown in Table 1. In contrast, both the hydrazine and hydraulic oil containing elements in A08 were open, with all hydrazine and most of the hydraulic oil lost. The hydrazine elements suffered severe damage, while the hydraulic element component damage was generally limited to tubing and flex lines. Table 2 gives a summary of damage received by individual components within the TVC subsystem, and Figure 2 shows a general view of the A08 TVC subsystem.

TABLE 1. A07 TVC SUBSYSTEM DAMAGE

| Item | Condition |
|--|----------------------------|
| A. Rock (left side) | |
| 1. Fuel Isolation Valve | Shock mount ring separated |
| 2. Fuel Supply Module Insulation | Lower two-thirds missing |
| 3. Fuel Supply Module, Impact Shield | Bracket broken |
| 4. Fuel Isolation Valve Inlet/Outlet Hoses | Kinked |
| 5. Fuel Supply Module and Reservoir Connectors | Heat Damage |
| B. Tilt (right side) | |
| 1. Fuel Supply Module Impact Shield | Bracket broken |

TABLE 2. A08 TVC SUBSYSTEM DAMAGE

| Item | Condition |
|--|--------------------|
| A. Rock (left side) | |
| 1. Low-Pressure Relief Valve (3/8 Dia) | Ruptured |
| 2. Low-Pressure Crossover Line (1-1/2 Dia) | Fractured |
| 3. Hydrazine Fill Line (1/4 Dia) | Pulled from Boss |
| 4. Fuel Feedline Hose (1/2 Dia) | Pulled from APU |
| 5. APU Purge in and out Flex Lines | Ruptured |
| 6. APU Fuel Pump | Ruptured |
| 7. Fuel Valve | Damaged |
| 8. Filter to Fuel Supply Module | Ruptured |
| 9. Fuel Supply Module Overflow | Ruptured |
| 10. Water Impact Deflector Brackets | Broken |
| 11. Reservoir Outlet Line | Flattened |
| B. Tilt (right side) | |
| 1. Low-Pressure Relief Line (3/8 Dia) | Ruptured |
| 2. Filter to Fuel Supply Module | Ruptured |
| 3. Fuel Supply Module Fill Line (1/4 Dia) | Pulled from Boss |
| 4. Feed Flex Lines | Separated from APU |
| 5. APU Fuel Pump | Disintegrated |
| 6. Fuel Valve | Damaged |
| 7. Actuator Crossover Return | Impacted |
| 8. Fuel Isolation Valve | Ruptured |

ORIGINAL PAGE
BLACK AND WHITE PHOTOGRAPH

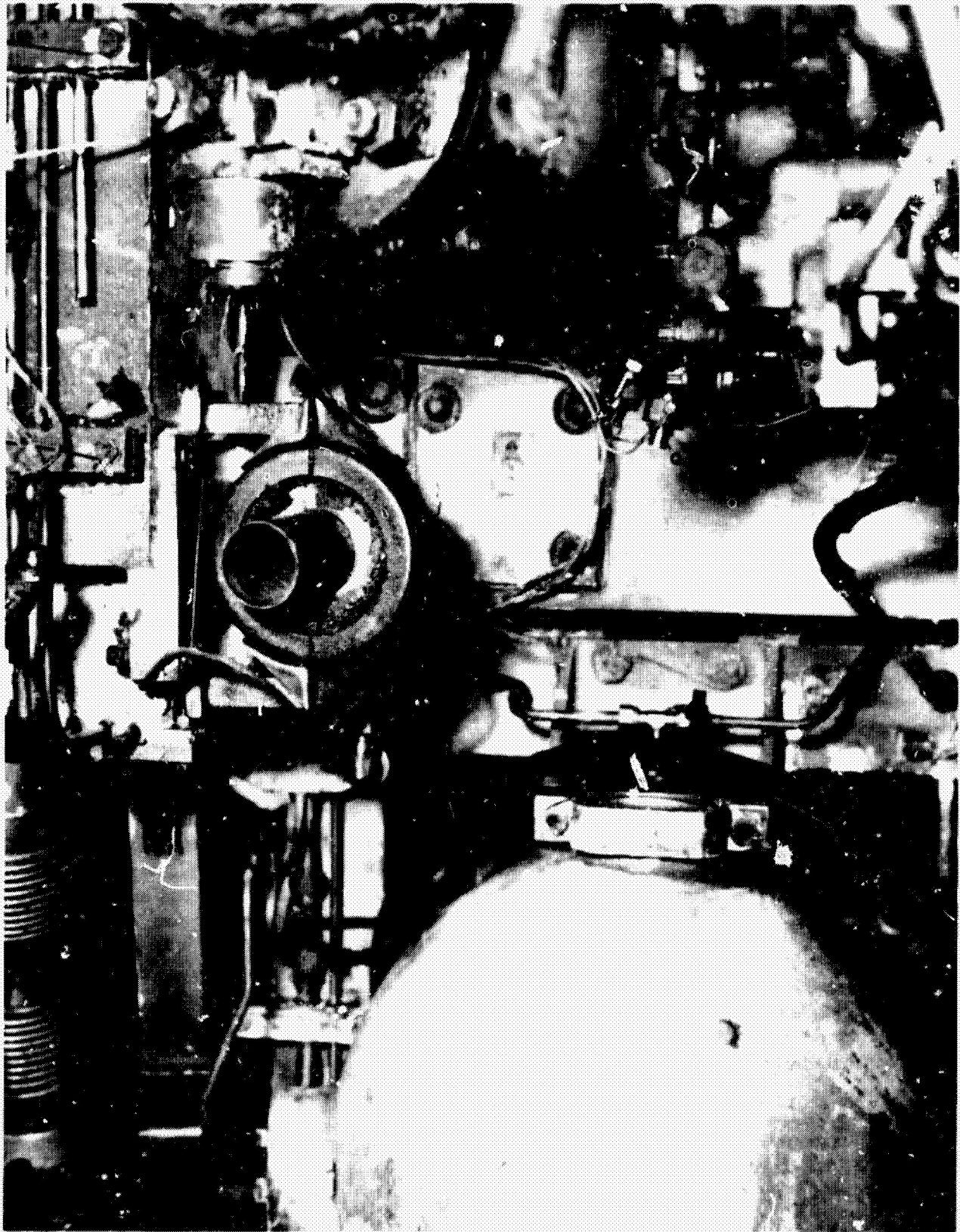


Figure 2. A08 VC subsystem damage.

B. Aft Skirt Structural Damage

Figures 3 and 4 chart the specific damage received by A07 and A08 aft skirts, respectively. This damage is further described below.

1. Rings. The most obvious and perhaps the most significant SRB damage was sustained by the structural rings on the interior of the aft skirt. Damage was generally similar in both skirts, and this damage may be characterized as follows:

- a. Forward Ring. Local damage to the inboard aft side of the flange of the ring.
- b. Intermediate Ring. Severe damage to nearly all of the ring except that portion immediately behind the TVC subsystem.
- c. Aft Ring. Extensive cracking in the outer flange at the ring web.

Figures 5 and 6 show views of the damage sustained by the intermediate ring. In all instances, the damage incurred by the rings appeared to be the result of a forward acting, longitudinal force; i.e., all damaged structure which was still attached was deformed in a forward direction. In addition, the fractures appeared to be very brittle¹ with little apparent yielding or plastic deformation evident.

Other damage noted was: (1) A07 actuators impacted the inboard flange of the intermediate rings causing partial shearing of the inboard ring flange, and (2) one longitudinal skin stiffener on A07 between the intermediate and forward rings was cleanly sheared off at the skin line, apparently the result of a secondary impact by a large piece of intermediate ring web which was missing in the same area. A number of ring-reinforcing gussets were completely missing from the intermediate ring in areas where the ring web was also missing. Some gusset fasteners were neatly sheared off at the interface between the gusset and the skin stringer to which they were attached. Perhaps, the most mystifying structural damage noted was a through crack, approximately 15 in. long, on the inner flange of the aft ring.

2. Thermal Curtain. As expected and per design intent, the thermal curtain was destroyed at the completion of the mission. The only remaining pieces of the thermal curtain were the shredded ends of the curtain segments under both the aft skirt and nozzle compliance ring retainers (Fig. 7). Also observed in the aft skirt area was that two thermal curtain retainers on the nozzle compliance ring were missing on each SRB and that these were missing prior to the reentry smudging of the aft skirt interior. These two retainers were immediately adjacent to the initiation point of the nozzle linear shaped charge. Figure 8 shows a view of the A08 nozzle compliance ring and shows the obvious discoloration of the paint due to reentry smoke. One other thermal curtain retainer segment was missing on the A07 compliance ring, located approximately 90 degrees counterclockwise from the nozzle initiation point (as viewed looking forward). The surface under this retainer segment, however, was clean, indicating the segment was lost after reentry smudging – presumably at water impact.

1. Later microscopic examination of the fractures showed the failures to be ductile while metallurgical analysis of the material in static tensile tests showed limited ductility (1 to 4 percent) in the short transverse direction.

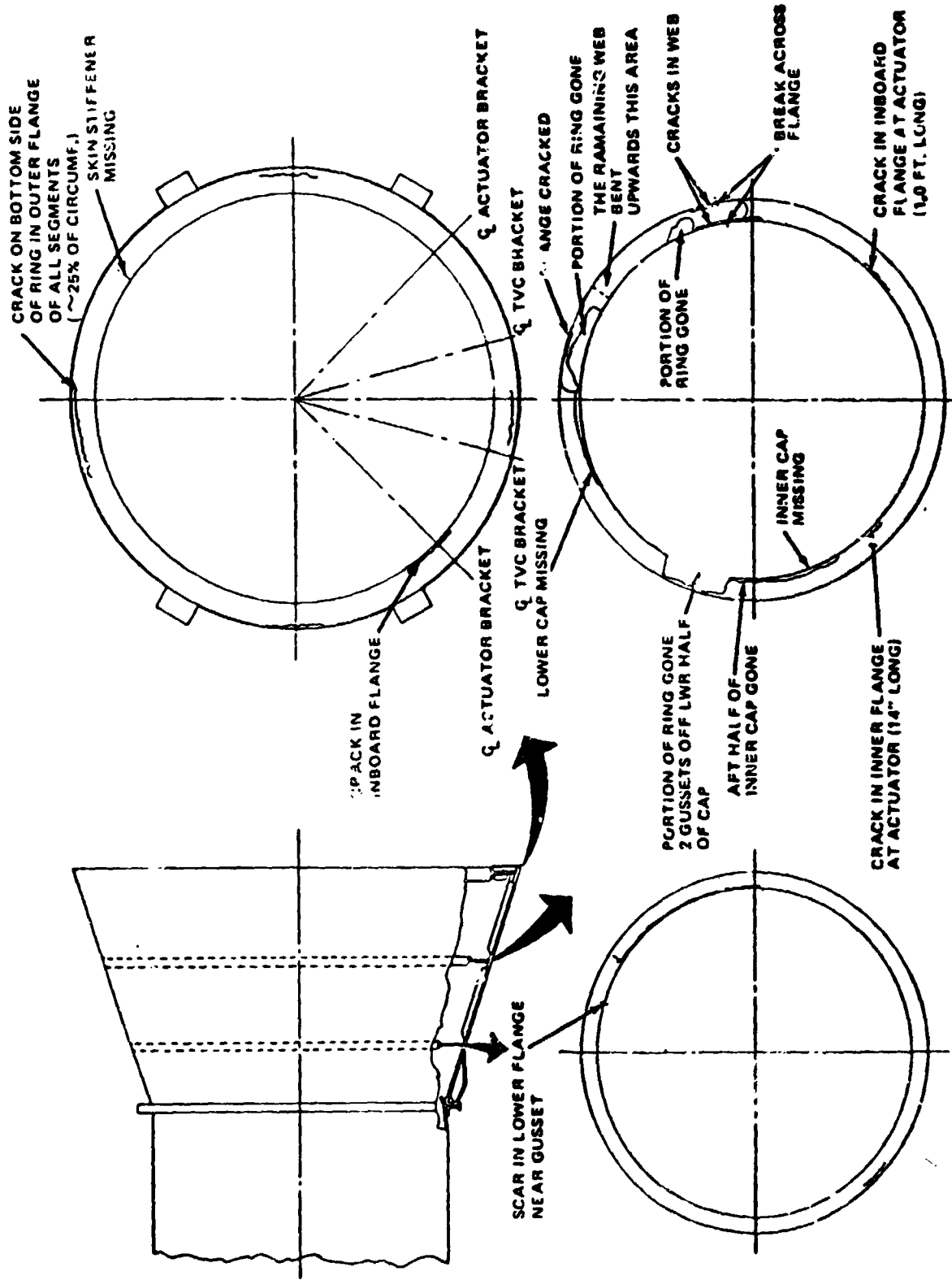


Figure 3. STS-1 aft skirt damage (A07).

ORIGINAL PAGE
BLACK AND WHITE PHOTOGRAPH



Figure 5. Intermediate ring damage.

ORIGINAL PAGE
BLACK AND WHITE PHOTOGRAPH

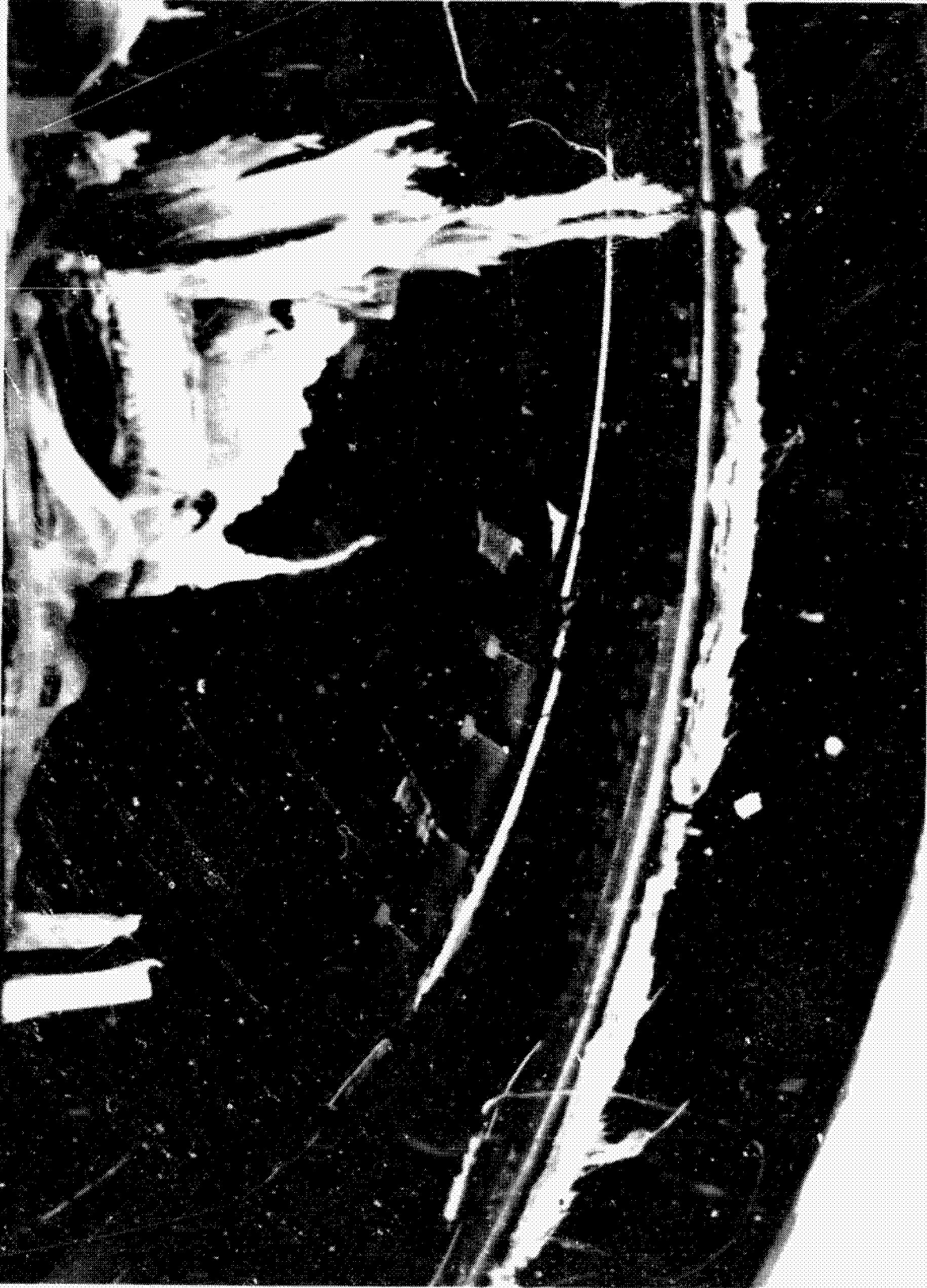


Figure 6. Intermediate ring damage.

ORIGINAL PAGE
BLACK AND WHITE PHOTOGRAPH

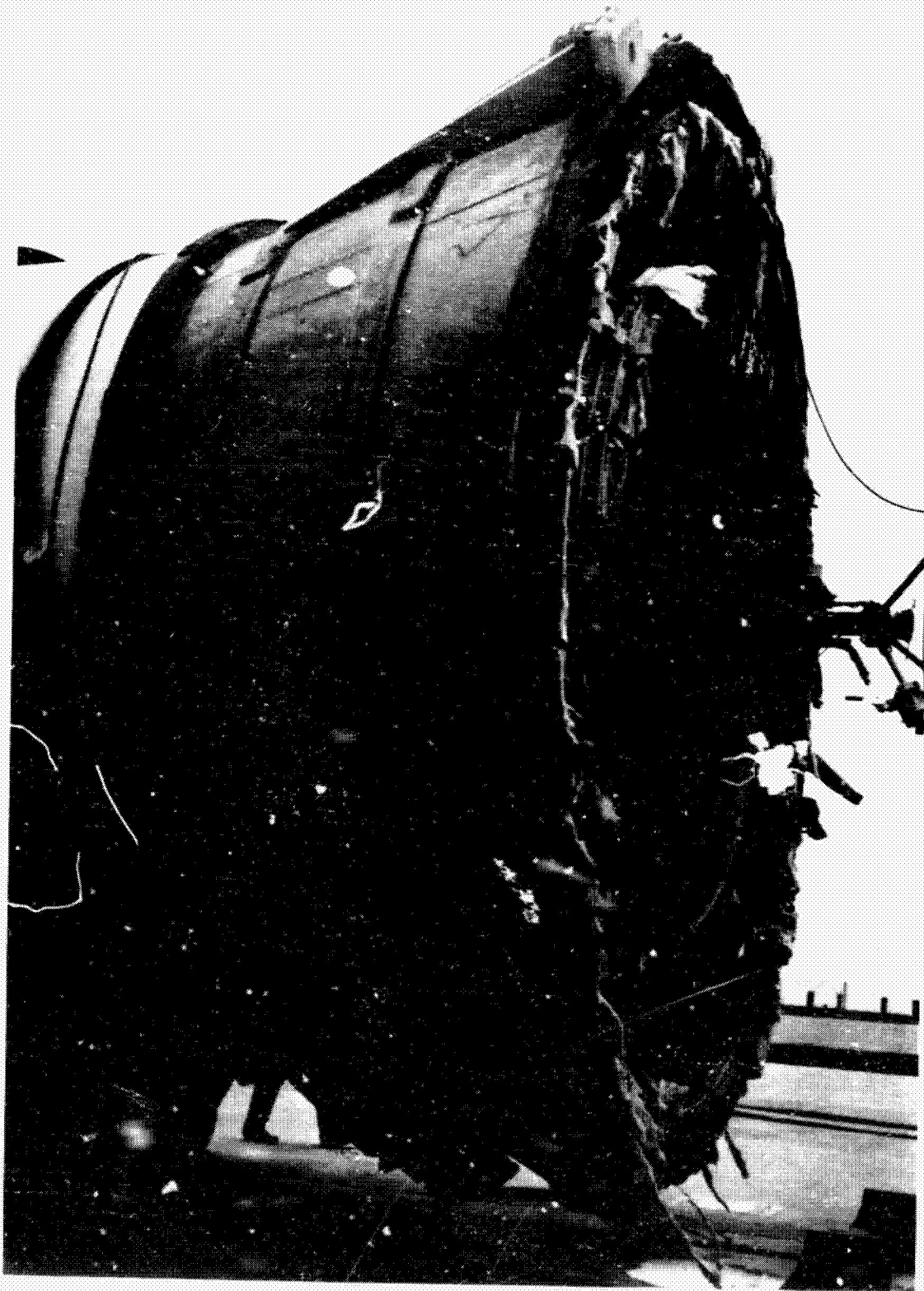


Figure 7. Thermal curtain remains.

ORIGINAL PAGE
BLACK AND WHITE PHOTOGRAPH

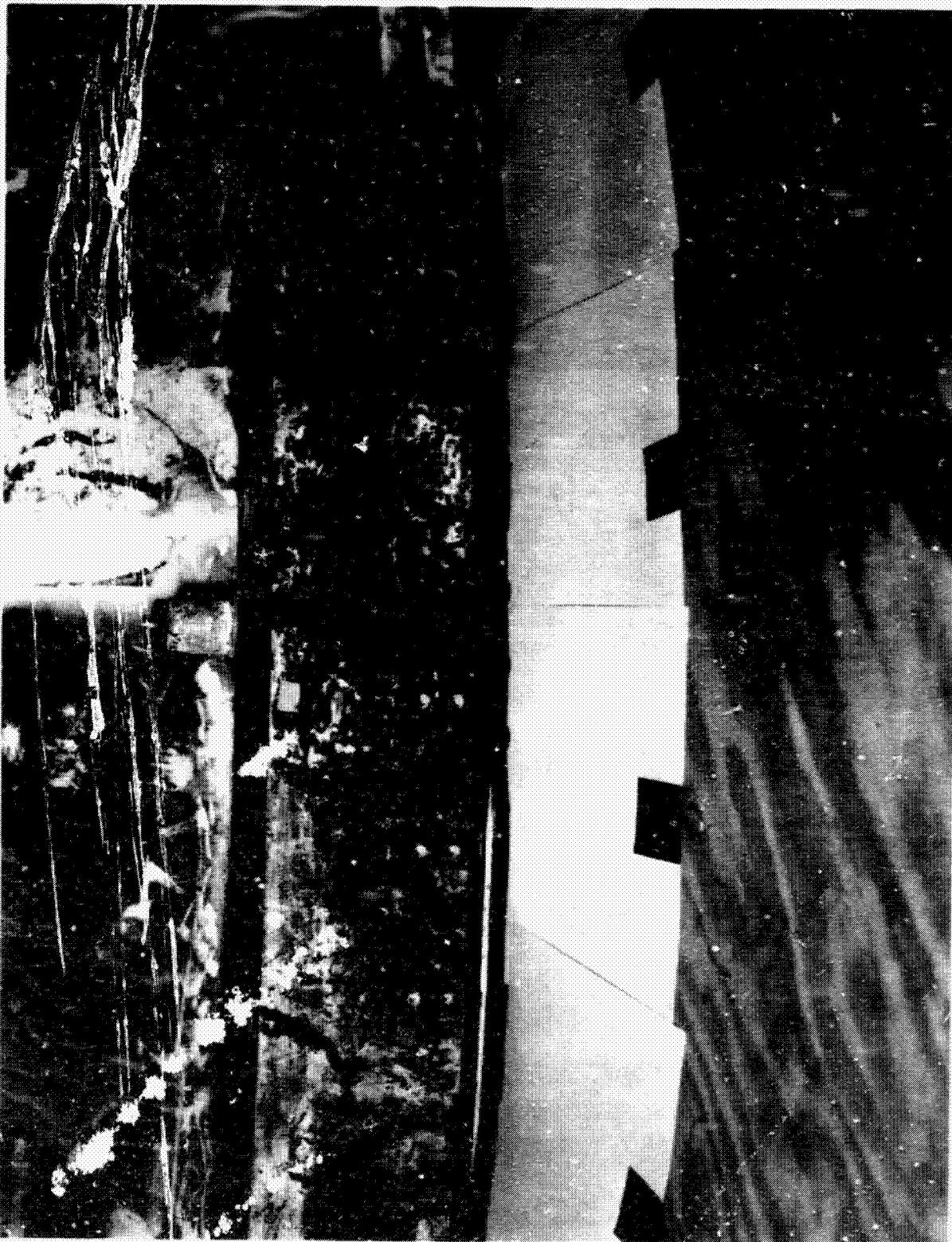


Figure 8. Missing thermal curtain retainers.

C. SRM Structural Damage

1. SRM Nozzle. The SRM nozzles exhibited some damage which was germane to the investigation of the overall aft skirt damage scenario, and this section will be limited to describing that damage observed in the aft exit cone area. Other damage in the forward nozzle area was identified and investigated by Thiokol and will not be discussed in this report.

The nozzle on the A07 (LH) booster sustained the greater damage. Both actuator attachment brackets were fractured and broken loose from the nozzle exit cone shell on A07, while the brackets were intact and undamaged on A08. Investigation by Thiokol also revealed local fractures in the aft cone shell in the vicinity of the actuator bracket attachment on A07, while the exit cone shell on A08 was undamaged.

The compliance rings on the nozzles appeared to be undamaged upon initial inspection, but a more detailed inspection later revealed some helicoils pulled out where the thermal curtain retainers were fastened [5]. This damage was common to both the A07 and A08 compliance rings and matched the locations where the thermal curtain retainers were missing, i.e., adjacent to the nozzle severance linear shaped charge initiation point.

2. SRM Case. As with the SRM nozzle, the ad hoc committee's interest in the SRM case was limited to evidence which might contribute to understanding of the SRB aft skirt damage. In this regard, the damage incurred by the aft segments of the SRM case was investigated to define the severity of the water impact loads. There was a significant difference in damage to the two cases [6], and these will be described separately.

a. A07 Case Segments. The LH SRM sustained the more severe damage of the two recovered motor cases. The damage from water impact was confined to the two aft most case segments, i.e., the two 120-in.-long segments between SRB station 1577.48 and SRB station 1817.60. In the forward most segment, a depression or "oil-canned" area of approximately 2 ft by 3 ft was sustained in the 0.50-in.-thick skin between the stiffener stubs. In the aft stiffener segment, 35 bolts were missing between the forward stub and the stiffener tee, and 28 bolts were missing between the aft stub and the stiffener tee. The tee stiffener itself was locally displaced forward from the flange approximately 1.0 in. All of the above damage was centered at approximately 270 degrees near the +Y axis. A later more detailed inspection also revealed radial cracks initiating at the stiffener attachment holes in the stub flanges.

b. A08 Case Segments. The RH case segment damage was confined to stiffener ring attachments in the aft most segment. The forward attachment had 27 bolts missing and the tee stiffener was locally displaced forward, as in A07, for about 1.0 in. In the aft attachment, 19 bolts were missing between the stiffener and the attachment stub. The A08 case damage was centered at approximately 135 degrees or midway between the +Z and the +Y axes. Figure 9 shows a photograph of the forward stiffener ring on A08.

FLIGHT DATA

Members of the ad hoc committee reviewed all flight data which could provide inputs to the investigation. Unfortunately, some key instrumentation failed to provide useful data, and this greatly hampered further analyses in some areas. Table 3 lists all of the measurements which were installed

ORIGINAL PAGE
BLACK AND WHITE PHOTOGRAPH

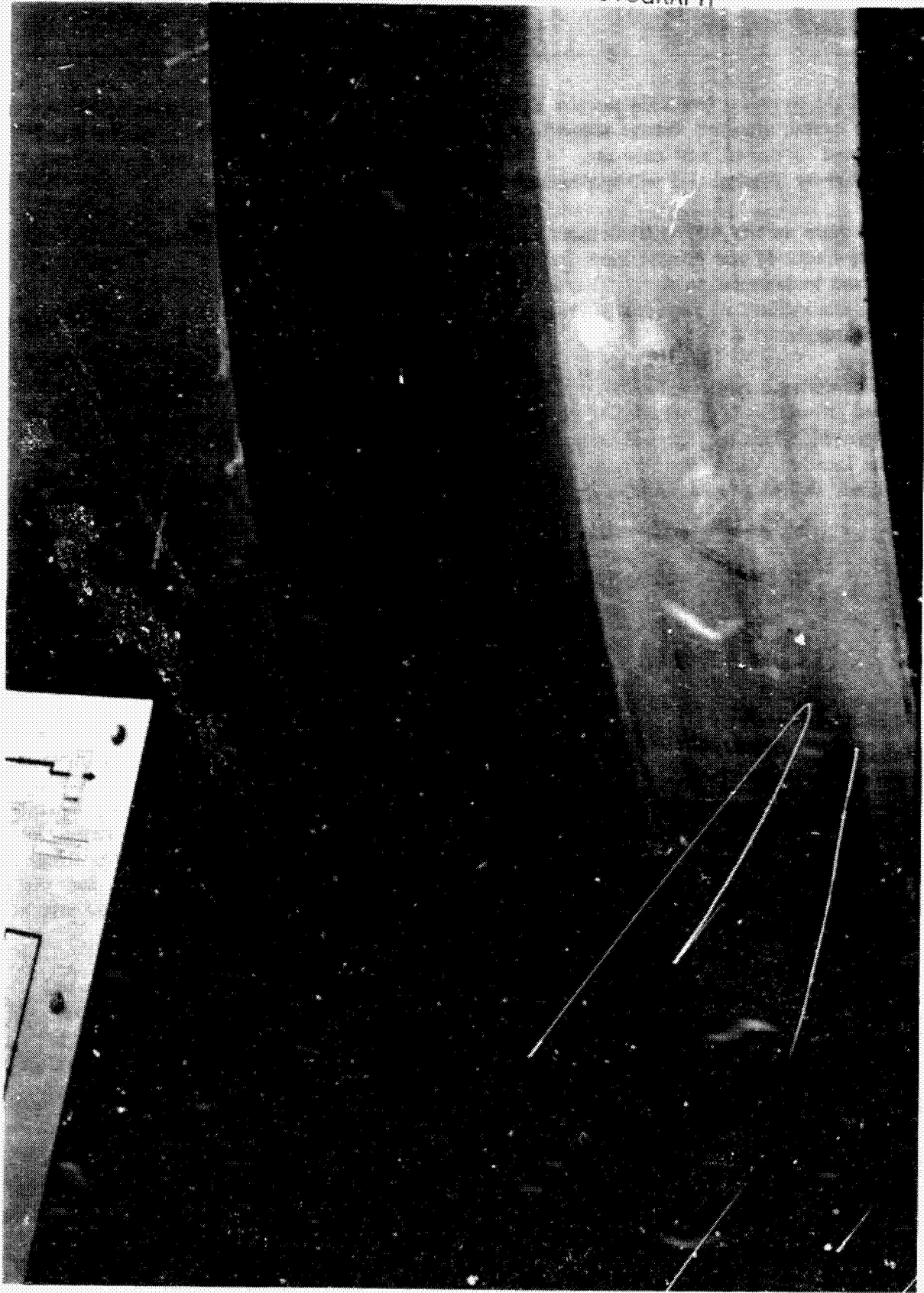


Figure 9. SRM forward stiffener ring (A08).

TABLE 3. SRB MEASUREMENTS LOST DURING REENTRY

| MSID | Description | Lost | Note |
|-----------|--|---------|------|
| B08D8092A | Vib -- Aft Sepn Motor, Radial Dir. | 330 Sec | (2) |
| B08D8121A | Vib -- Input to TVC Lower Frame, Rad Dir | 350 Sec | |
| B08D8122A | Vib -- Input to TVC Lower Frame, Flt Dir | 340 Sec | |
| B58P8300A | Press -- Diff. Tilt Servo Actr. | 340 Sec | |
| B08P8303A | Press -- Ext. Static, Fwd Skirt 2 | 340 Sec | (1) |
| B08P8305A | Press -- Ext. Static, Fwd Skirt 4 | 340 Sec | |
| B08P8314A | Press -- Engine Nozzle, Ext. 2 | 340 Sec | (2) |
| B08P8330A | Press -- Aft Skirt, Ext. 1 | 340 Sec | (2) |
| B08P8332A | Press -- Aft Skirt, Ext. 3 | 340 Sec | (2) |
| B07P8350A | Press -- Ascent, Ext. to Heat Shield 1 | 338 Sec | (2) |
| B07P8351A | Press -- Ascent, Ext. to Heat Shield 2 | 335 Sec | (2) |
| B07P8352A | Press -- Ascent, Ext. to Heat Shield 3 | 335 Sec | (1) |
| B07P8353A | Press -- Ascent, Ext. to Heat Shield 4 | 335 Sec | (2) |
| B07P8359A | Press -- Ascent, Int. to Heat Shield 1 | 330 Sec | |
| B07P8360A | Press -- Ascent, Int. to Heat Shield 2 | 330 Sec | (2) |
| B07P8361A | Press -- Ascent, Int. to Heat Shield 3 | 330 Sec | (2) |
| B07P8362A | Press -- Ascent, Int. to Heat Shield 4 | 335 Sec | (2) |
| B07R8401A | Heat Flux -- Radiation, Aft Skirt 1 | 320 Sec | (2) |
| B07R8402A | Heat Flux -- Radiation, Aft Skirt 2 | 340 Sec | (2) |
| B07R8403A | Heat Flux -- Radiation, Aft Skirt 3 | 340 Sec | (2) |
| B07R8404A | Heat Flux -- Radiation, Aft Skirt 4 | 340 Sec | (2) |
| B07R8405A | Heat Flux -- Radiation, Aft Skirt 5 | 340 Sec | (2) |
| B07R8407A | Heat Flux -- Total, Aft Skirt 1 | 343 Sec | (2) |
| B07R8408A | Heat Flux -- Total, Aft Skirt 2 | 342 Sec | (2) |
| B07R8409A | Heat Flux -- Total, Aft Skirt 3 | 336 Sec | (2) |
| B07R8434A | Heat Flux -- Total, Aft Skirt 4 | 333 Sec | (2) |
| B07R8435A | Heat Flux -- Total, Aft Skirt 5 | 340 Sec | (2) |
| B07R8436A | Heat Flux -- Total, Aft Skirt 6 | 330 Sec | (2) |
| B07R8449A | Heat Flux -- Total, Int. Aft Skirt 1 | 338 Sec | (1) |
| B07T8474A | Temp -- Aft Skirt, Mid Top Outboard | 340 Sec | (2) |
| B07T8475A | Temp -- Aft Skirt, Mid Top Inboard | 330 Sec | (2) |
| B07T8476A | Temp -- Aft Skirt, Mid Bottom Inboard | 334 Sec | (2) |
| B07T8477A | Temp -- Aft Skirt, Mid Inboard | 330 Sec | (2) |
| B07T8478A | Temp -- Aft Skirt, Aft Inboard | 330 Sec | (2) |
| B58T8507A | Temp -- Hydraulic Fluid, Syst. A | 340 Sec | |
| B58T8508A | Temp -- Hydraulic Fluid, Syst. B | 340 Sec | |
| B07T8509A | Temp -- Aft Skirt, Int. Top | 340 Sec | (1) |
| B07T8510A | Temp -- Aft Skirt, Int. Inboard | 340 Sec | (1) |
| B07T8511A | Temp -- Aft Skirt, Int. Bottom | 330 Sec | (1) |
| B07T8512A | Temp -- Aft Skirt, Int. Outboard | 330 Sec | |
| B07T8527A | Temp -- Cable Raceway, Fwd | 330 Sec | (2) |
| B46T8534A | Temp -- APU A Turbine Exhaust | 330 Sec | (1) |
| B46T8535A | Temp -- APU B Turbine Exhaust | 330 Sec | |
| B08Y8982A | Acou. -- Aft Skirt, Ext. No. 1 | 335 Sec | (2) |

Notes: (1) Comparable measures failed on other SRB.
(2) No comparable measure on other SRS.

TABLE 3. (Concluded)

| MSID | Description | Lost | Note |
|-----------|---|---------|------|
| B08Y8984A | Acou. - Aft Skirt Heat Shld. Int. No. 1 | 331 Sec | |
| B08Y8985A | Acou. - Aft Skirt Heat Shld, Int. No. 2 | 332 Sec | |
| B08Y8986A | Acou. - Aft Skirt Shld, Int. | 334 Sec | |
| B07R7449A | Heat Flux - Total, Int. Aft Skirt 1 | 338 Sec | (1) |
| B07R7450A | Heat Flux - Total, Int. Aft Skirt 2 | 340 Sec | (1) |
| B07T7470A | Temp. - Aft Skirt, Fwd Bot Inboard 1 | 347 Sec | (2) |
| B07T7471A | Temp. - Aft Skirt, Fwd Bot Inboard 1 | 347 Sec | (2) |
| B07T7473A | Temp. - Aft Skirt, Fwd Bot Inboard 2 | 395 Sec | (2) |
| B07T7509A | Temp. - Aft Skirt, Int. Top | 350 Sec | (1) |
| B07T7510A | Temp. - Aft Skirt, Int. Inboard | 332 Sec | (1) |
| B07T7511A | Temp. - Aft Skirt, Int. Bottom | 337 Sec | (1) |
| B46T7534A | Temp. - APU A Turbine Exhaust | 330 Sec | (1) |

Notes: (1) Comparable measures failed on other SRB.
 (2) No comparable measures on other SRS.

on the STS-1 boosters and failed during the early stages of atmospheric reentry. This section summarizes the status of data as determined by the STS-1 Flight Evaluation Working Group and documented in the Final Flight Evaluation Report [7].

A. Significant Event Times

Table 4 gives a summary of STS-1 times for significant events as extracted from the STS-1 Final Flight Evaluation Report.

B. Reentry Thermal Data

Reentry heating within the aft skirt cavity was of special interest, and a limited amount of valuable data was obtained prior to sensor malfunctions [8].

1. Calorimeters. SRB reentry aerodynamic heating for STS-1 was measured by ascent calorimeters only, since reentry DFI calorimeters will not be installed until STS-3. The ascent calorimeters were not sized for reentry, nor were they located appropriately for determining reentry heating. However, valuable insight into the performance of the SRB thermal curtain was obtained by comparing calorimeter data from a sensor exposed directly to the external heat flux (facing aft) to a sensor within the aft skirt cavity (i.e., behind the thermal curtain). Figure 10 shows the former, for the RH SRB and Figures 11 and 12 show the latter for the LH and RH SRB, respectively. It is apparent that the thermal curtain was able to provide excellent thermal insulation prior to 200 sec, but afforded little or no protection upon encountering reentry aerodynamic heating at approximately 300 sec.

TABLE 4. °RB SIGNIFICANT EVENT TIMES

| Item | Event Description | Source | Time from Ref (sec) | |
|------|--|------------|---------------------|-----------|
| | | | Actual | Predicted |
| 1. | Liftoff | SRM Thrust | 1.183 | 1.205 |
| 2. | SRB Separation | B57P7311A | 131.826 | 132.403 |
| 3. | LH Nozzle Jettison | B52X7847E | 202.875 | 202.5 |
| 4. | RH Nozzle Jettison | B52X8897E | 203.016 | 202.5 |
| 5. | Reentry Max q | Estimated | 341.0 | 334.0 |
| 6. | LH High Altitude Baroswitch Closed (LH Nose Cap Jettison) | 852X7880E | 369.004 | 360.0 |
| 7. | RH High Altitude Baroswitch Closed (RH Nose Cap Jettison) | B52X8880E | 371.343 | 360.0 |
| 8. | LH Low Altitude Baroswitch Closed (LH Frustum Separation) | B55V1618A | 391.491 | 382.0 |
| 9. | RH Low Altitude Baroswitch Closed (RH Frustum Separation) | B55V2618A | 393.793 | 382.0 |
| 10. | LH SRB Impact | B52X7886E | 424.915 | 426.0 |
| 11. | RH SRB Impact | B52X8886E | 428.052 | 426.0 |

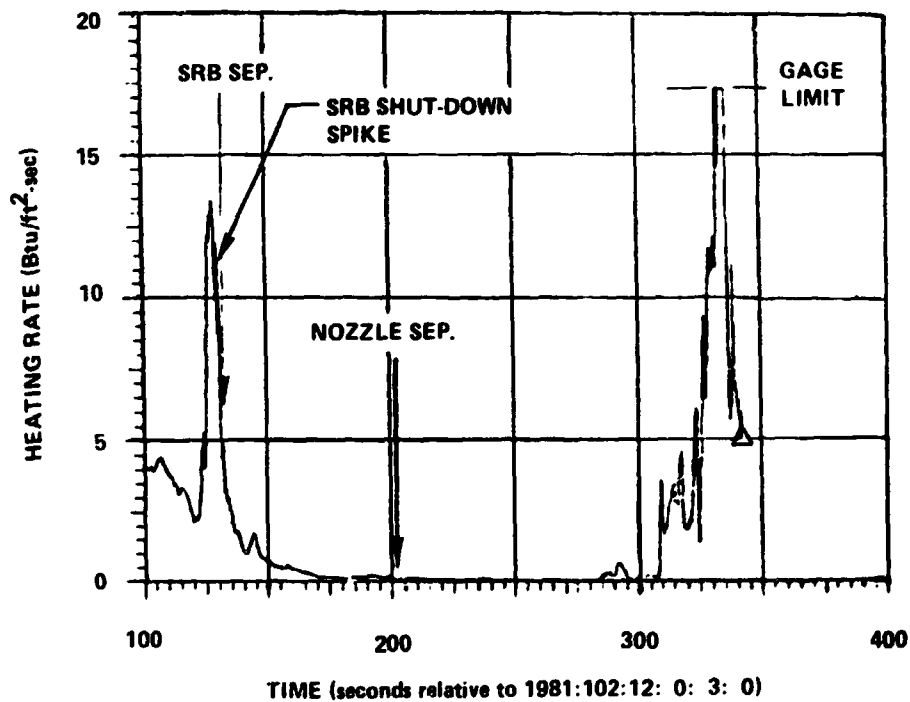


Figure 10. Aft skirt heating rate (A08).

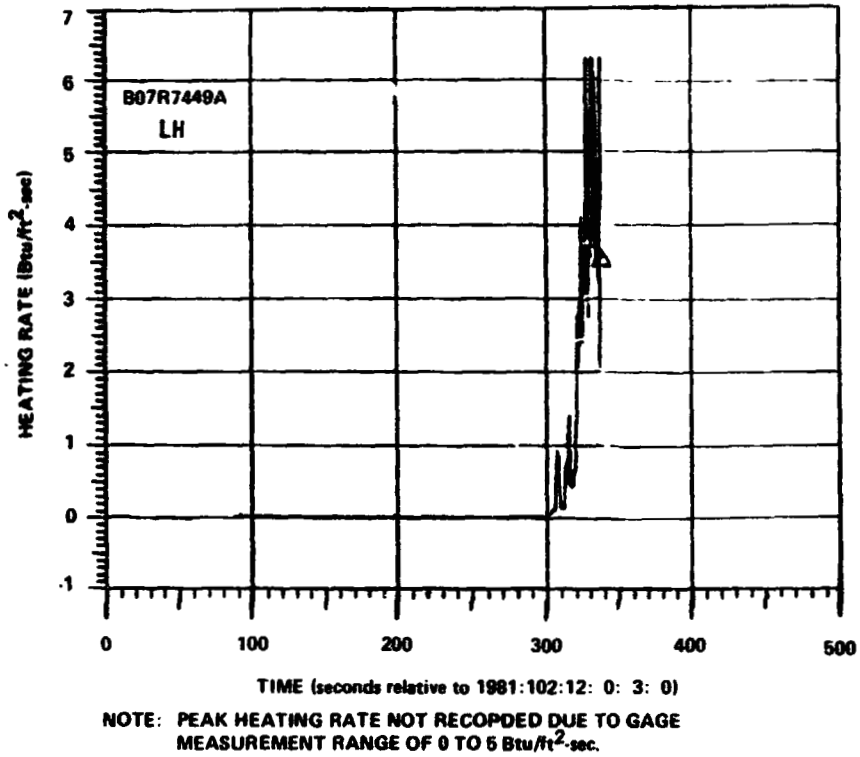


Figure 11. Internal aft skirt heating rate (A07).

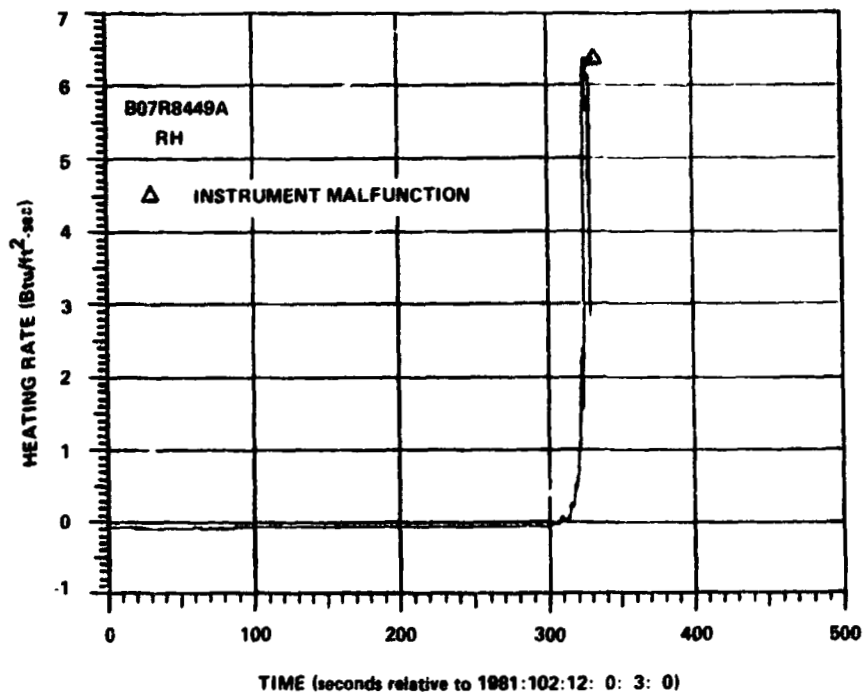


Figure 12. Internal aft skirt heating rate (A08).

**ORIGINAL PAGE IS
OF POOR QUALITY**

2. Thermocouples. The SRB aft skirt structural temperatures were recorded by a total of 17 thermocouples mounted on the interior of the aft skirts. Table 5 summarizes the locations for both the LH and RH boosters. The response of thermocouples located on the aft skirt skins is shown in Figures 13 and 14. In addition, the STS-1 preflight nominal temperature prediction has been plotted for one thermocouple which is designated by the darkened symbol (Δ) on each figure. Also shown is a second comparison curve with the predicted temperature at the same location if the thermal curtain were lost prior to the maximum reentry heating. Figures 15 and 16 show similar data for the aft ring frames in the LH and RH SRB, respectively.

With two exceptions, all thermocouple data were lost between 330 and 345 sec (the two surviving thermocouples are, however, still suspect after 350 sec). The loss of data is believed to be caused by the progressive physical damage of DFI cables as described earlier in this report.

TABLE 5. STS-1 AFT SKIRT STRUCTURAL TEMPERATURE MEASUREMENTS

| Measurement No. | X_B | θ | Description | Number |
|-----------------|-------|----------|--------------------|--------|
| LHSRB | | | | |
| B07T7470A | 1877 | 90 | Skin | 1 |
| B07T7471A | 1877 | 135 | Skin | 2 |
| B07T7473A | 1877 | 166 | Skin | 3 |
| B07T7509A | 1926 | 358 | Aft Ring Frame Web | 1 |
| B07T7510A | 1926 | 90 | Aft Ring Frame Web | 2 |
| B07T7511A | 1926 | 187 | Aft Ring Frame Web | 3 |
| B07T7512A | 1926 | 270 | Aft Ring Frame Web | 4 |
| RHSRB | | | | |
| B07T8474A | 1910 | 45 | Skin | 1 |
| B07T8475A | 1877 | 315 | Skin | 2 |
| B07T8476A | 1910 | 225 | Skin | 3 |
| B07T8477A | 1910 | 265 | Skin | 4 |
| B07T8512A | 1927 | 273 | Skin* | N/A |
| B07T8509A | 1926 | 358 | Aft Ring Frame Web | 1 |
| B07T8510A | 1926 | 90 | Aft Ring Frame Web | 2 |
| B07T8511A | 1926 | 180 | Aft Ring Frame Web | 3 |
| B07T8478A | 1926 | 270 | Aft Ring Frame Web | 4 |

*Beneath instrument island.

3. Passive Temperature Sensors. Passive temperature sensors were applied to the aft skirt interior structure prior to the STS-1 launch. These stick-on sensors were applied to record the maximum local structural temperatures during the mission. Table 6 shows the maximum temperatures recorded by the sensors for various locations; however, the data is suspect, and is judged to be not indicative of the actual structural temperatures. There was ample evidence showing the sensors to be responding to gas temperature following the failure of the thermal curtain.

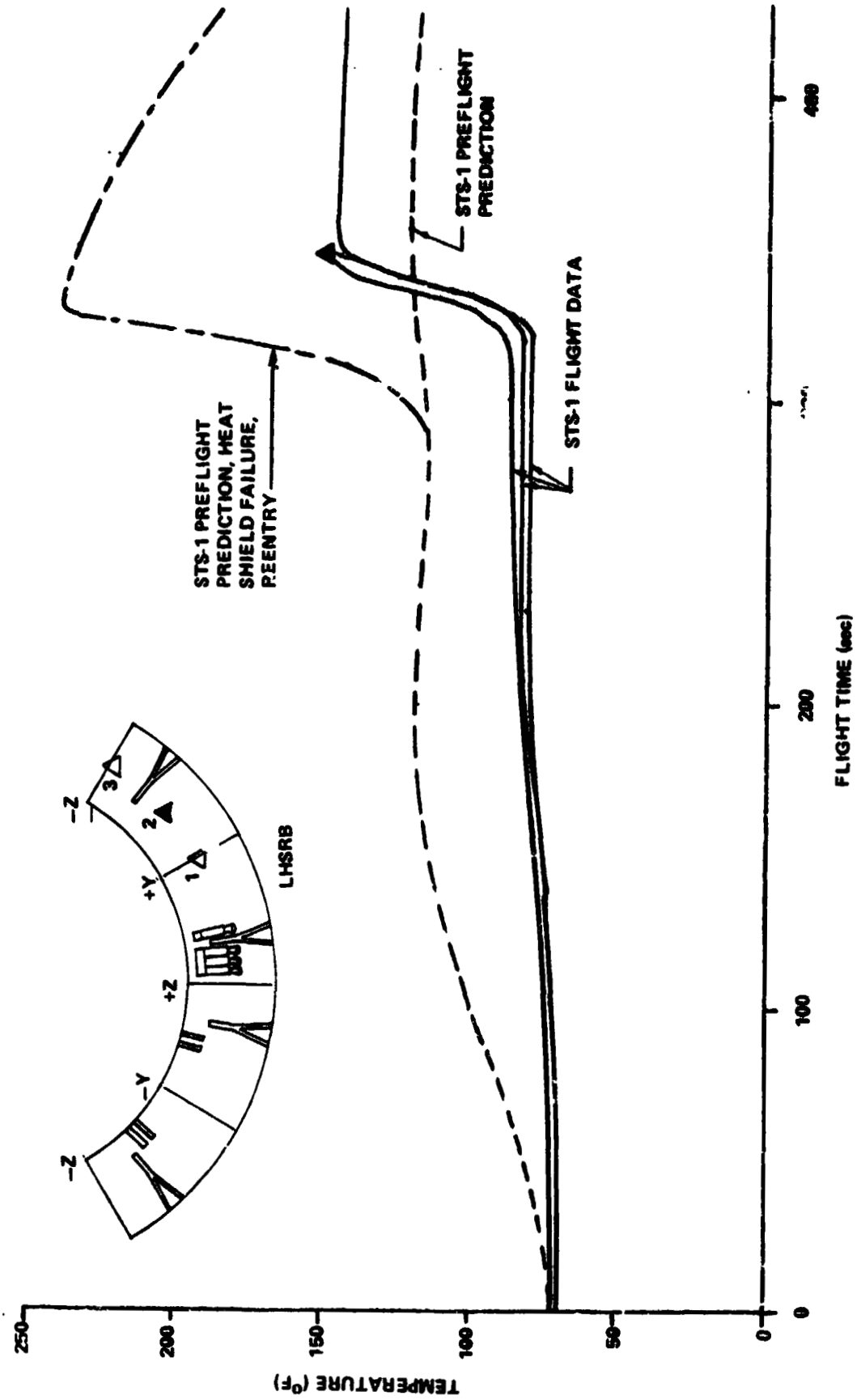


Figure 13. Aft skirt skin temperatures (A07).

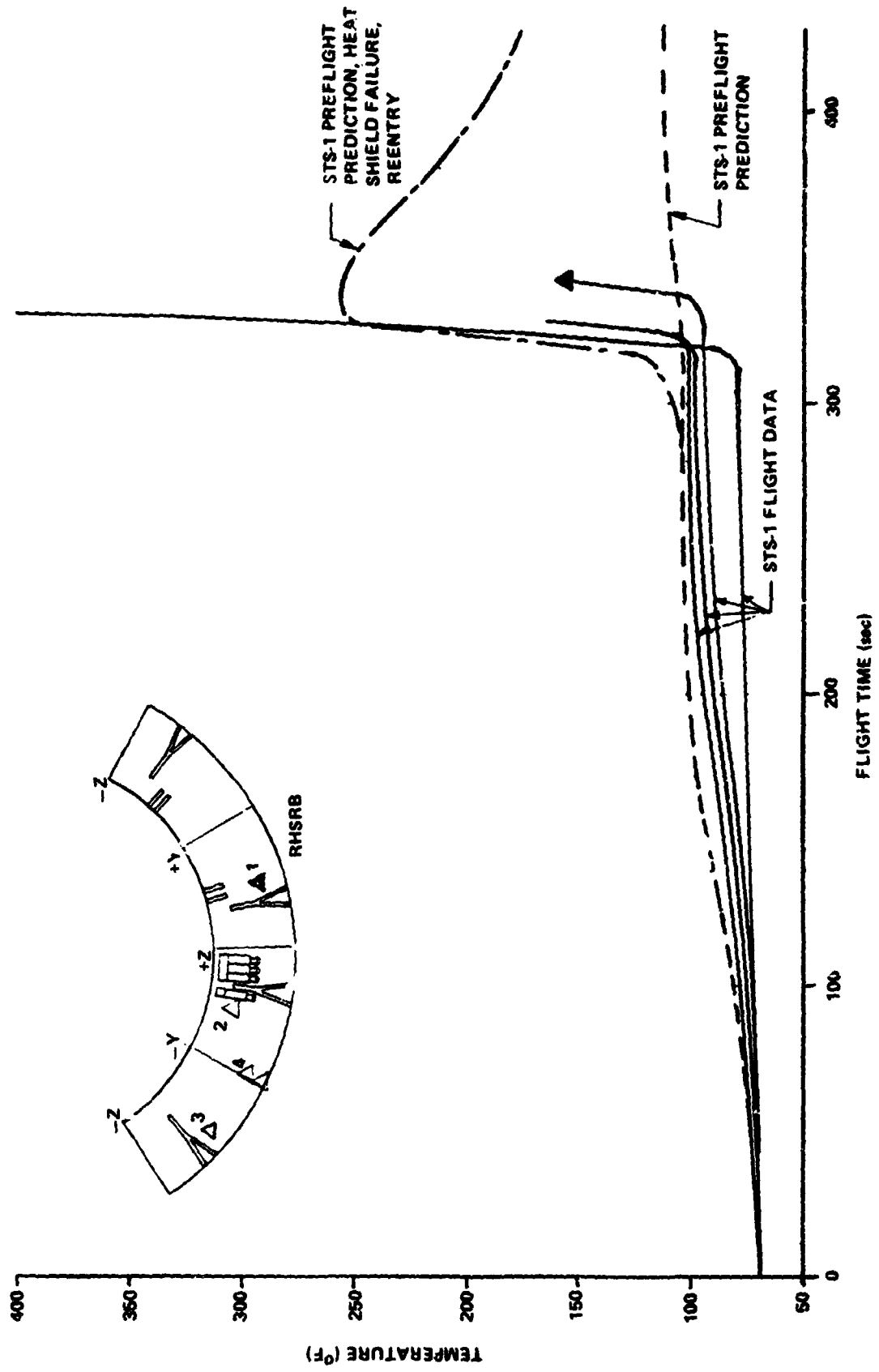


Figure 14. Aft skirt skin temperatures (A08).

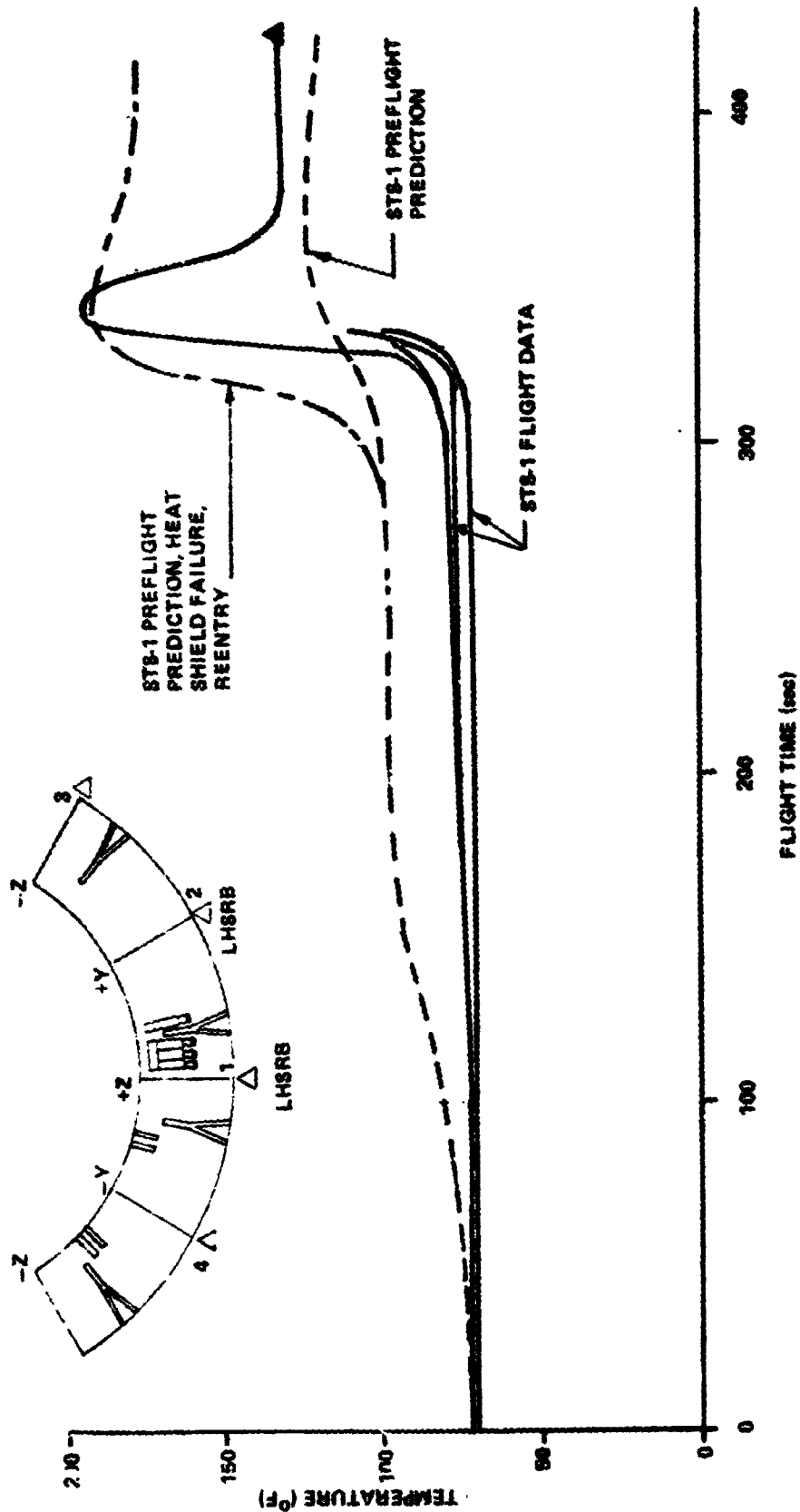


Figure 15. Aft skirt aft ring frame temperatures (A07).

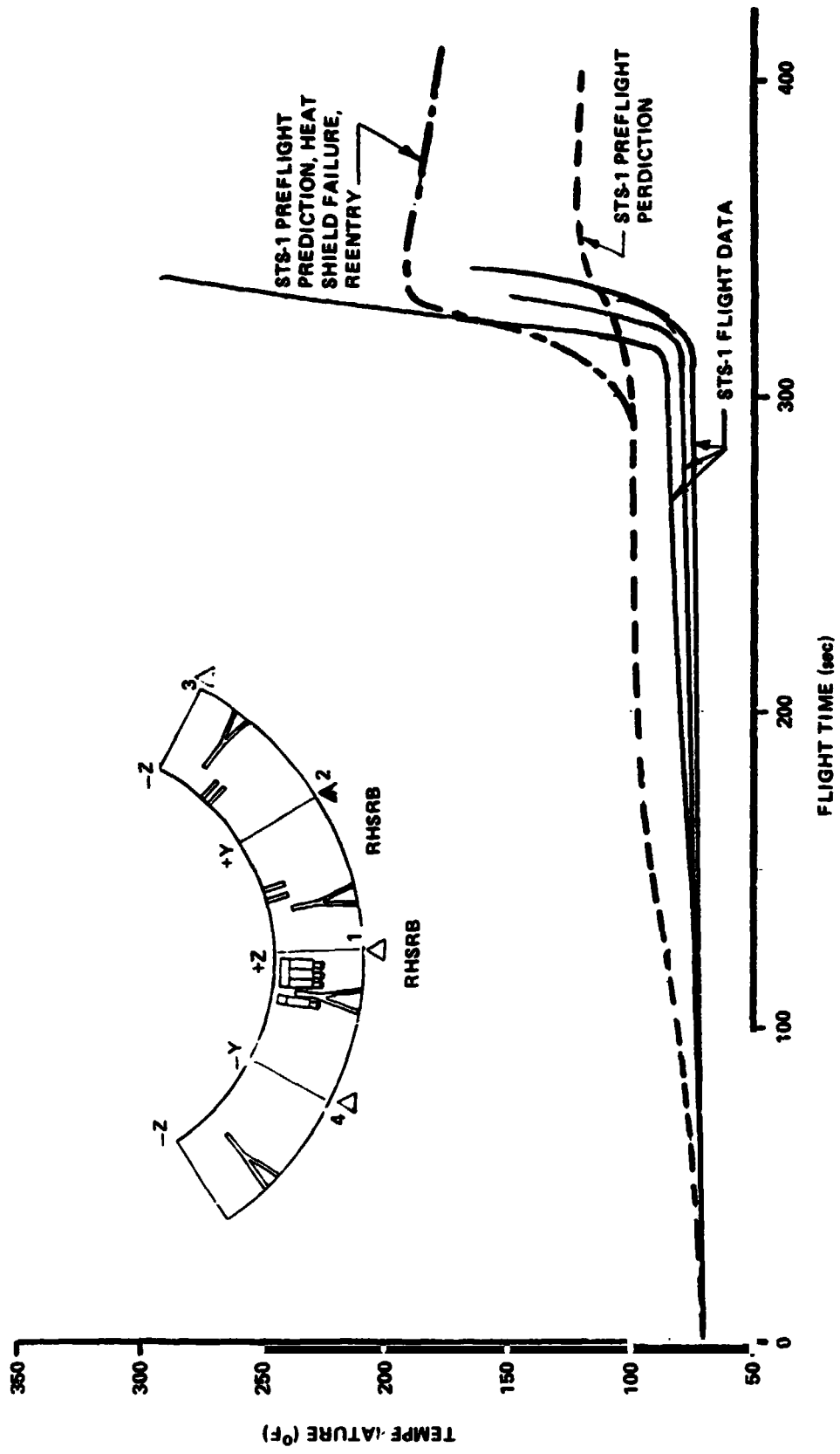


Figure 16. Aft skirt aft ring frame temperatures (A08).

TABLE 6. DATA FROM PASSIVE TEMPERATURE SENSORS

| Parameter | Aft Skirt | |
|--------------------------------|--|---|
| | A07 | A08 |
| ● Loss Due to Burnout | 30% | 50% |
| ● Primary Loss Zone | $X_B = 1910$ Aft $\theta = 45^\circ$ to 315° | $X_B = 1877$ Aft $\theta = 0^\circ$ to 135° |
| ● Maximum Temperature Recorded | | |
| – Skin | 310°F ($\theta = 315^\circ$) | 390°F ($\theta = 135^\circ$) |
| – Ring Frame Web | 290°F ($\theta = 0^\circ$) | 395°F ($\theta = 135^\circ$) |
| – Stiffener Flange | 290°F ($\theta = 0^\circ$) | 375°F ($\theta = 225^\circ, 315^\circ$) |
| – Stiffener Web | 290°F ($\theta = 0^\circ$) | 400°F ($\theta = 225^\circ$) |

- Passive temperature sensors responding to gas temperature.
- Not indicative of structural temperature.

4. SRM Instrumentation. Instrumentation on the SRM nozzle was of interest in assessing the presence of SRM afterburning during reentry. Two sensors (B07R8410A and B078411A) on the RH SRB nozzle near the exit plane show total heat flux to have tailed off from an average of 3.0 Btu/ft² sec in the 130 to 135 sec time frame to approximately 0 Btu/ft² sec at 167 sec and remained there until nozzle severance, at which time the instrumentation is disabled [9].

5. Reentry Film. Color, 70 mm movies were taken of SRB reentry from the tracking ship USNS Vandenberg with long telephoto lenses. A 120-in. camera was trained on A07 between 361 sec after liftoff and water impact, and a 180-in. cinetelescope camera recorded the A08 reentry between 247 sec and water impact with only two short (4 to 5 sec) lapses. The SRB reentry films were of interest thermally in that they clearly showed the burning in the aft skirt cavity during a portion of the atmospheric entry. The color of the flames, the color of the smoke, and the time the fire was observed were all valuable evidence in determining the cause of the fire. A bright orange fire and thick black smoke were visible in the reentry films beginning near the time of nose cap jettison, 368 sec after lift-off, at about 16,000 ft altitude. The smoke and flame were substantially gone by the time of frustum separation at 393 sec (6,000 ft altitude).

C. Water Impact Loads Data

As noted previously, much instrumentation was lost during the early reentry phase. This was particularly true for those sensors dealing with water impact loads. Some limited data of a gross nature was obtained and this is described in the following.

1. Accelerometers. Both axial and lateral accelerations were obtained for both boosters. From visual interpretation of oscillographs, the events at water impact can be generally reconstructed as follows: The maximum axial loads occurred during the initial impact phase with maximum accelerations for both A07 and A08 of 14 to 16 g. Maximum lateral loads, in the order of 8 to 10 g,

occurred at both initial impact and cavity collapse. In addition, the lateral accelerations give some indications as to the direction of loading: approximately in the $-Y$ direction for A07 and midway between the $-Y$ and $-Z$ axes for A08.

2. Pressure Transducers. Pressure transducers to measure water impact pressures in the aft skirt were located only in the RH (A08) booster. None of these measurements survived the early aerodynamic reentry phase (Table 3), so no local pressure data was obtained.

3. SRM Instrumentation. Pressure transducers were located on the aft SRM segments at SRB stations 1637 and 1765 (i.e., on the SRM case wall between the stiffener stub flanges). These circumferential arrays of pressure transducers provided good data for defining direction and magnitude of cavity collapse loads on the motor case. Figure 17 shows this data along with a reconstructed cavity collapse pressure profile for the RH booster (A08).

Another valuable SRM measurement was the internal motor case pressure during water impact. Figures 18 and 19 give the time history of the motor case internal "ullage" pressure, and show the significant pressure drop at water impact in both boosters. This pressure drop is caused by the rapid cooling of the internal gasses by water spray through the nozzle. This pressure drop, 10 psi below ambient for A07 and 7 psi below ambient for A08, adds directly to the cavity collapse pressure loading on the case exterior. The measurements are also of interest as an indicator of the internal ullage gas temperature at water impact.

4. Reentry Films. The reentry films, described earlier under Reentry Thermal Data, were also quite useful for water impact analysis. Approximate preimpact orientation of both boosters, both in angle relative to the velocity vector and the clocking angle, were determined from frame-by-frame analyses of the films.

POST FLIGHT ANALYSES

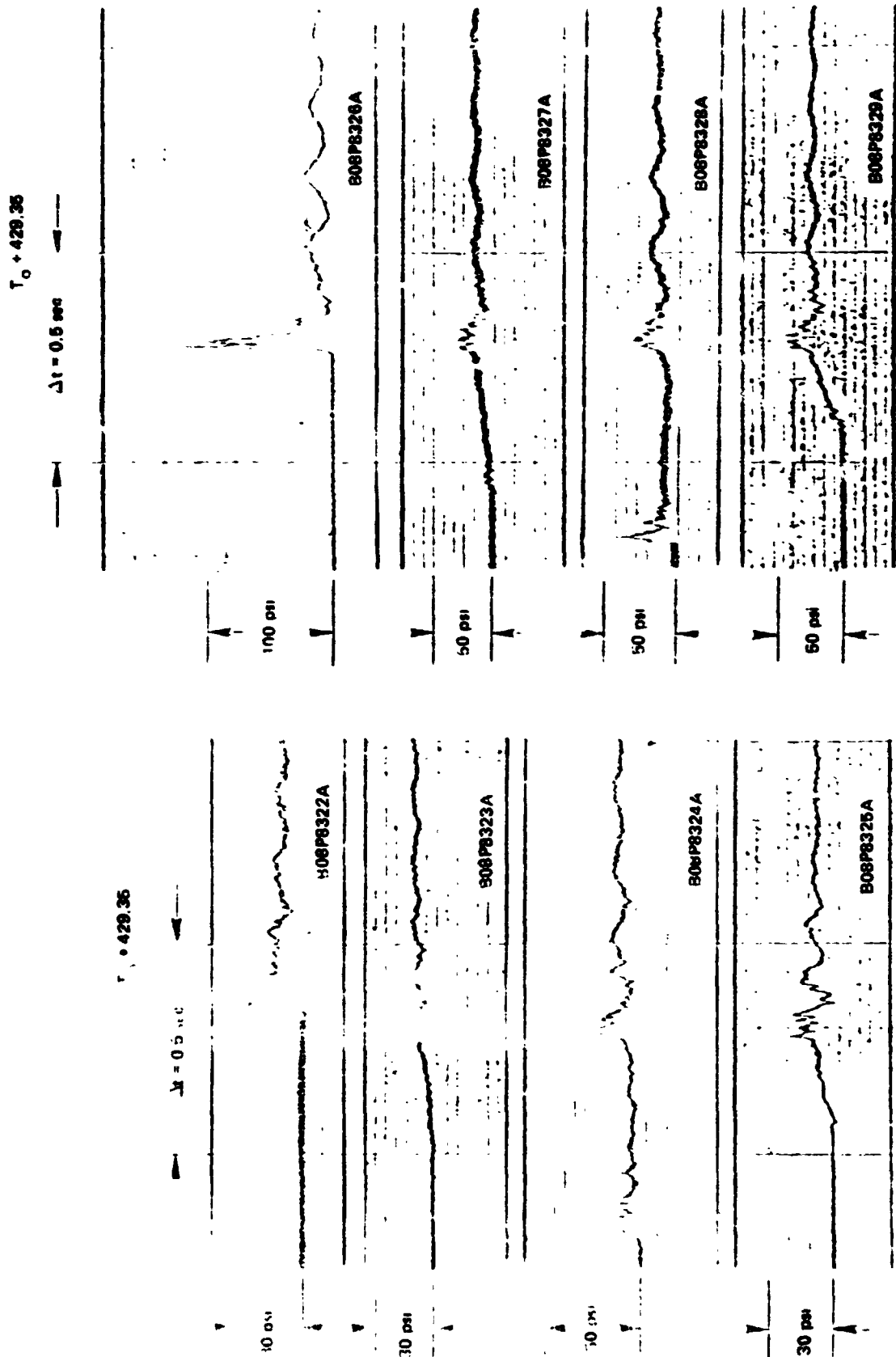
A number of postflight analytical studies and hardware failure analyses were performed to specifically identify the causes of the damage observed on STS-1 boosters. In general, these analyses: (1) showed that hypothesized events either could or could not have happened, (2) reconstructed actual flight events based on available data, or (3) predicted future flight events based on STS-1 experience. Some of the more significant postflight analysis results are given below.

A. Thermal Analyses

Thermal analyses were performed for the portions of the SRB aft skirt area to determine what sequence of events occurred that could have produced the fire related damage on STS-1.

1. Reentry Ignition Potential. Thiokol analysts evaluated the potential for SRM unburned propellants to ignite ("afterburning") upon reentry into the atmosphere [9]. In addition, the SRM internal insulation, liner, and nozzle ablatives were assessed as potential hydrocarbon fuels during reentry. The results of these analyses, as stated in Reference 9, show that SRM propellant afterburning did not occur, but either the nozzle ablatives or insulation and liner were a likely source of burning during reentry. Table 7 gives the composition of nozzle pyrolysis gas and Table 8 shows the inflammability limits of certain gasses. The Thiokol analysis also shows that ignition of the pyrolysis gasses should occur in the chamber prior to about 316 sec after lift-off.

ORIGINAL PAGE IS
OF POOR QUALITY



b) VEHICLE STATION 1785

a) VEHICLE STATION 1637

Figure 17. Cavity collapse pressures (A08).

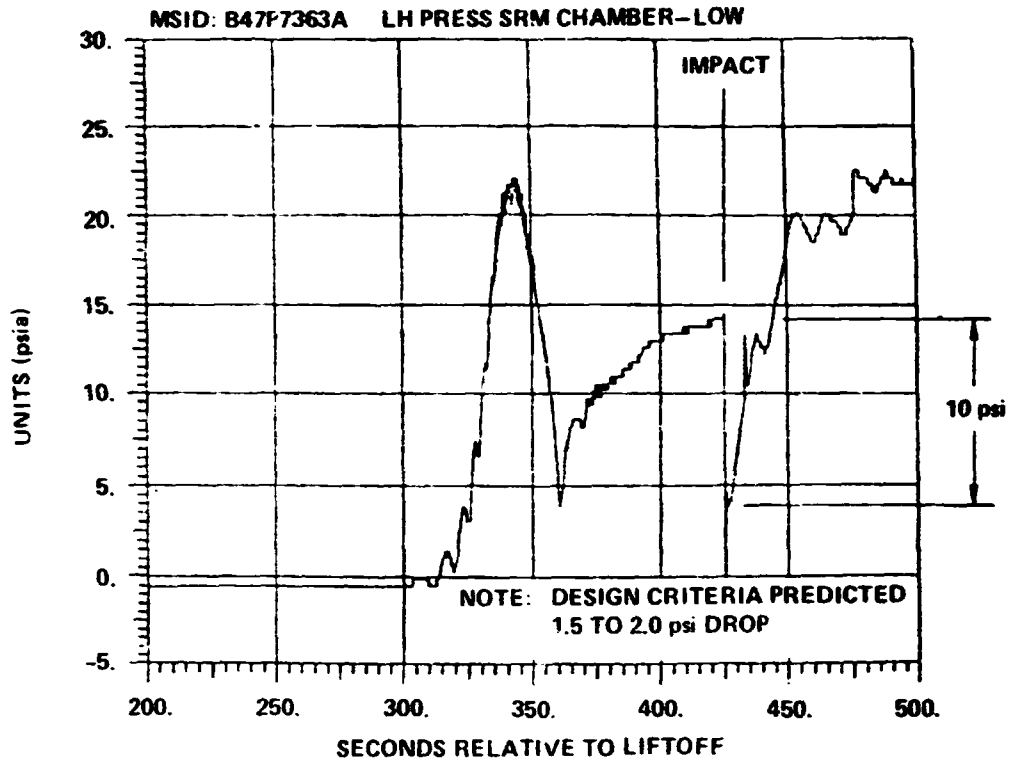


Figure 18. SRM internal pressure (A07).

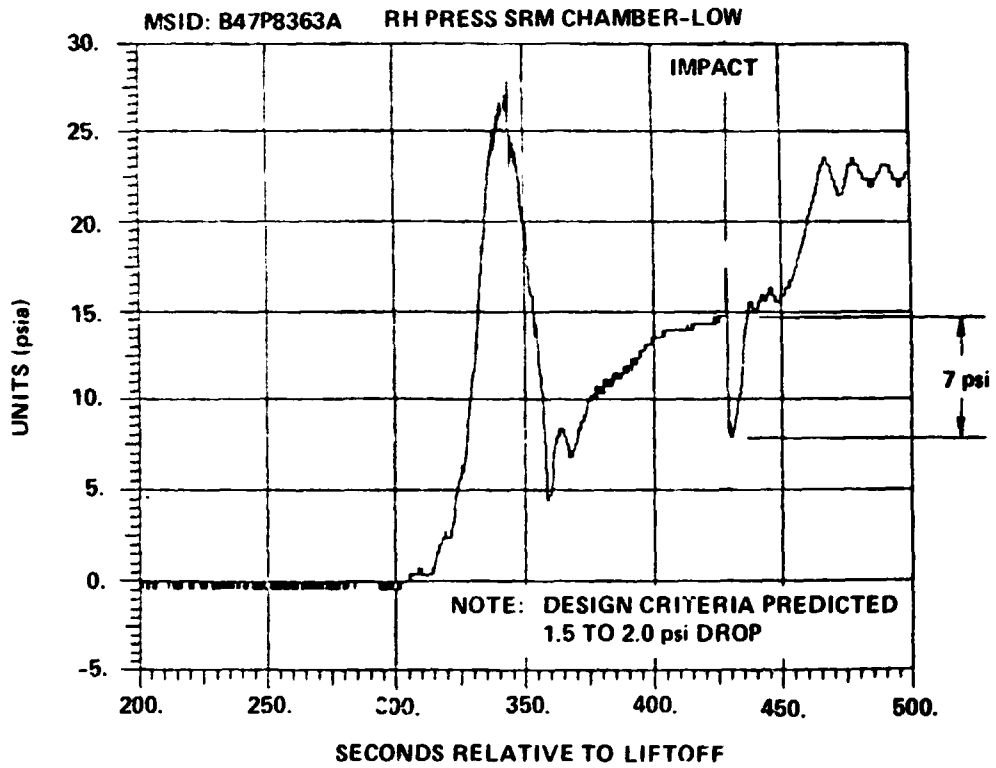


Figure 19. SRM internal pressure (A08).

TABLE 7. NOZZLE PYROLYSIS GAS COMPOSITION

| Specie | Formula | Mass Fraction | Mole Fraction |
|-------------------|----------------------------------|---------------|---------------|
| Carbon dioxide | CO ₂ | 0.3271 | 0.240 |
| Isopropyl alcohol | C ₃ H ₇ OH | 0.2044 | 0.110 |
| Methane | CH ₄ | 0.1635 | 0.329 |
| Carbon Monoxide | CO | 0.2617 | 0.302 |
| Acetylene | C ₂ H ₂ | 0.0025 | 0.0031 |
| Cyclohexane | C ₆ H ₁₂ | 0.0409 | 0.016 |

TABLE 8. INFLAMMABILITY LIMITS WITH AIR
(Atmospheric Pressure and Room Temperature)

| Specie | Formula | Limits of Inflammability (Volume Percent) | |
|-------------------|---------------------------------|--|-------|
| | | Lower | Upper |
| Methane | CH ₄ | 5.3 | 15.0 |
| Ethane | C ₂ H ₆ | 3.0 | 12.5 |
| Propane | C ₃ H ₈ | 2.2 | 9.5 |
| Isobutane | C ₄ H ₁₀ | 1.8 | 8.4 |
| Pentane | C ₅ H ₁₂ | 1.5 | 7.8 |
| Ethylene | C ₂ H ₄ | 3.1 | 32.0 |
| Acetylene | C ₂ H ₂ | 2.5 | 80.0 |
| Cyclohexane | C ₆ H ₁₂ | 1.3 | 8.0 |
| Isopropyl Alcohol | C ₃ H ₈ O | 2.0 | 12.0 |

2. Aft Skirt Components Temperatures. A reentry thermal analysis was performed assuming no thermal curtain between the SRM nozzle and the aft skirt aft ring [10]. Since the actual reentry orientation of the A07 and A08 boosters could not be determined, the predicted aerodynamic heating rates for these analyses were based on an assumed vehicle tumble profile. Four subsystem elements which suffered extensive damage on STS-1 were examined: (1) the TVC low pressure relief hydraulic line, (2) the hydrazine service line, (3) a shielded, waterproofed measurement cable, and (4) a shielded, nonwaterproof measurement cable routed to the actuator. Analytical results showed that the TVC low-pressure relief hydraulic line (titanium) had a predicted maximum temperature of 570°F, and the hydrazine service line (stainless steel) up to 440°F. The predicted temperatures could cause rupture of the lines (the relief line was ruptured on A08, no lines were ruptured on A07). Maximum predicted temperatures of the electrical cables ranged between 545°F and 740°F which is sufficient to produce the damage observed on A07 and A08 cables.

3. Nozzle Severance LSC Temperature. A thermal analysis was performed by Thiokol [11] to determine the temperature rise in the nozzle linear shaped charge if nozzle severance were delayed until just prior to water impact, i.e., the nozzle LSC would be subjected to reentry aerodynamic heating. The analysis indicated that there would be no thermal degradation nor autoignition hazard created by the additional heating, and, in fact, the predicted temperature rise at the LSC would be only 3°F. However, it was concluded that additional insulation would be required for protection of the initiator lead wire.

B. Structure Analyses

The aft skirt structure, in particular the three stiffener rings, was extensively analyzed to determine the intensity of the applied water pressure during splashdown which would be required to produce the damage seen on the STS-1 boosters. This loading was compared to the preflight predictions based on STS-1 initial water impact conditions as determined from scale model drop tests.

1. Water Impact Conditions. From analysis of films, the initial velocities and altitudes of both A07 and A08 boosters were estimated [7]. These conditions are shown in Table 9, with the coordinate and sign conventions illustrated in Figure 20. The water entry vertical velocity was determined to be significantly higher than the 88 ft/sec value predicted for STS-1 boosters as well as the 85 ft/sec design value. The horizontal velocity was estimated to be very small in comparison with the design value of 45 ft/sec and the impact angle was estimated to be approximately that used for design loads, i.e., $\theta = -5$ degrees.

TABLE 9. ESTIMATED WATER IMPACT CONDITIONS

| Parameter | Left SRB (A07) | Right SRB (A08) |
|-----------------------------|----------------|-----------------|
| Vertical Velocity - V_V | 93 fps | 94 fps |
| Horizontal Velocity - V_H | <5 fps | <5 fps |
| Impact Angle - θ | -3° to -7° | -3° to -7° |
| Roll Angle - ϕ | See Figure 21 | |

The roll angle or clocking angle orientation, as shown in Figure 21, showed the horizontal velocity vector to be in the -Y direction for A07 and approximately midway between the -Z and -Y axes for A08. Penetration depth of the boosters was significantly greater than preflight predictions, with a maximum initial depth of approximately 50 ft on both boosters compared to the design value of 40 ft. Both boosters stabilized in the spar buoy flotation mode, as predicted, with eventual freeboard during initial retrieval operations of 25 ft on A07 and 40 ft on A08.

2. Cavity Collapse Loads. The analysis of cavity collapse differential pressures on STS-1 boosters involved determination of both internal and external pressures during water impact. Using the pressure data from the eight pressure transducers at the two aft SRM stations described earlier in this report, a peak cavity collapse pressure of approximately 167 psig was determined at vehicle station 1765. Figure 22 shows the good comparison of the measured value with the peak pressure predicted for the STS-1 actual conditions. The analysis did show that the axial distribution of pressure was slightly more forward on the vehicle than predicted as shown in Figure 23.

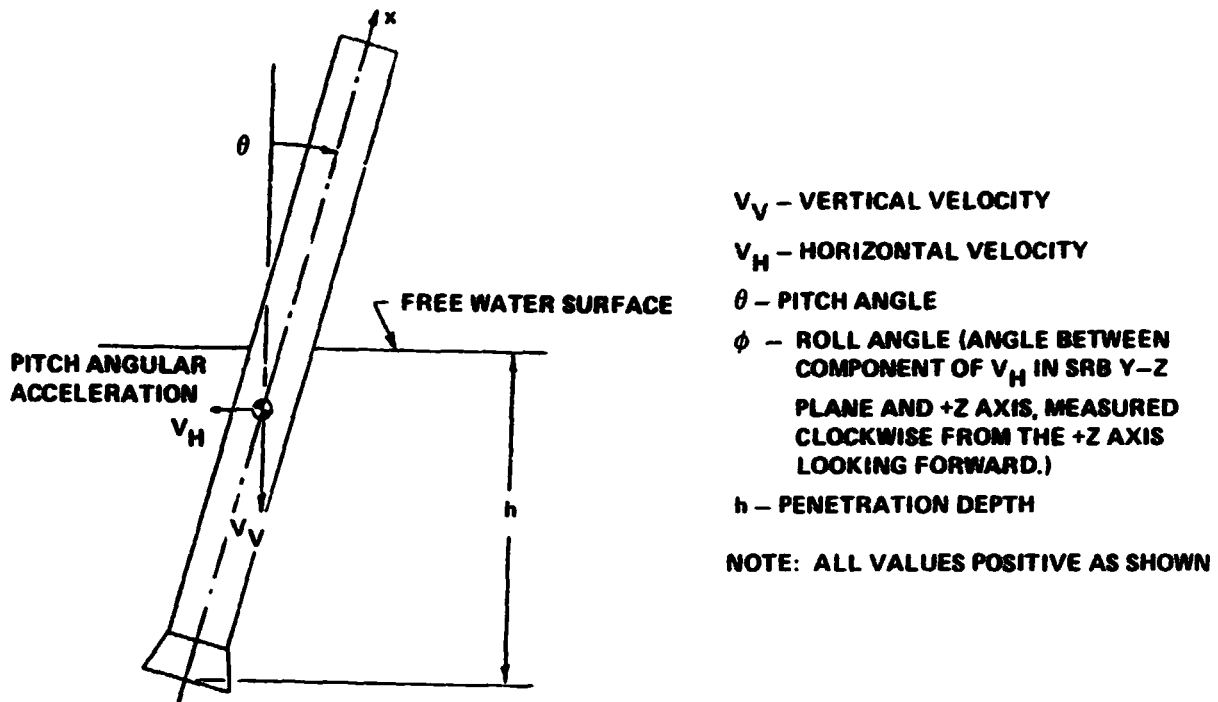


Figure 20. SRB water impact loads coordinate system and sign convention.

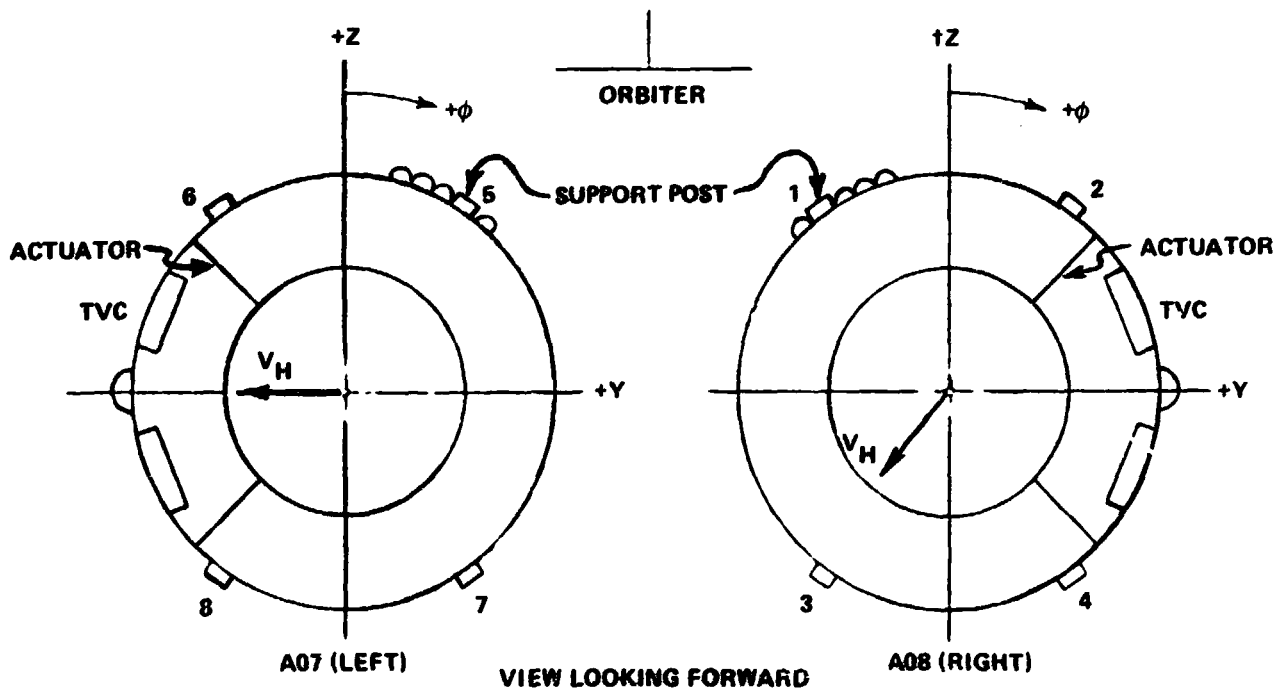


Figure 21. SRB roll orientations at water impact.

ORIGINAL PAGE IS
OF POOR QUALITY

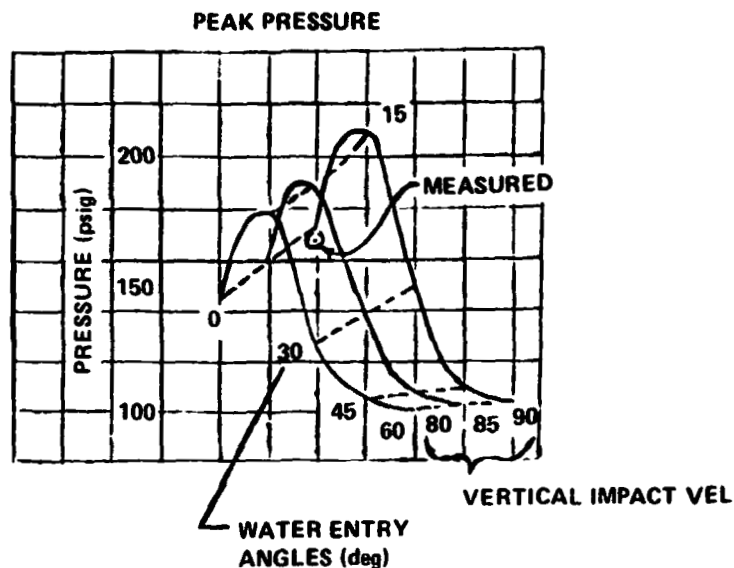


Figure 22. Cavity collapse peak pressure.

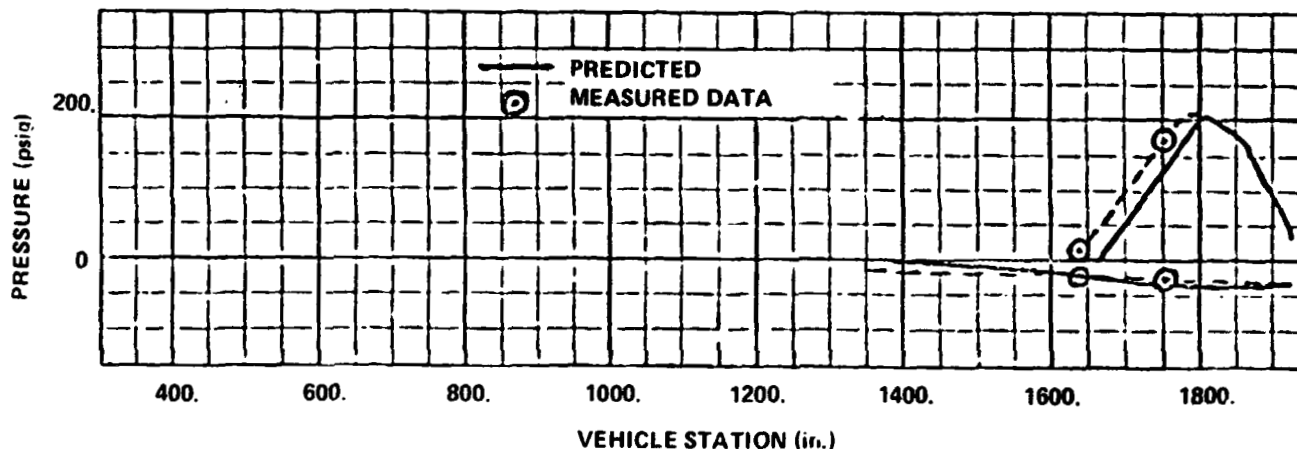


Figure 23. Cavity collapse pressure - longitudinal distribution (A08).

The internal SRM case pressures were analyzed from on-board measurements [12]. As illustrated in Figures 18 and 19, there was a significant pressure drop in both cases: 10 psi below ambient on A07 and 7 psi below ambient on A08. This pressure drop is greater than the 1.5 to 2.0 psi predicted as design criteria.

3. Aft Skirt Ring Stresses. A key question in the aft skirt investigation was what caused the structure failure of the ring frames. The STS-1 water impact conditions were somewhat different than predicted, so it was necessary to define a new set of applied loads on the aft skirt structure. Using the parametric water impact loads data derived from scale model drops, a revised set of loads, based on actual drop conditions, was defined and applied to the aft skirt structure. The resulting stresses were then computed to determine whether the damage observed on the aft skirts was likely to have happened at the specific STS-1 water entry conditions. The results of the analyses, given in Table 10 show that the ring damage should not have occurred at the specific STS-1 water entry conditions. The analyses used representative ring material properties based on postflight tests of specimens cut from the failed rings.

**TABLE 10. RESULTS OF POST-FLIGHT STRESS ANALYSIS
ON THE AFT SKIRT INTERMEDIATE RING**

| | Load Condition | | θ° | Web Pressure (psi) | Factor of Safety | |
|--|----------------|----------------|----------------|--------------------|------------------|-------|
| | V_V (ft/sec) | V_H (ft/sec) | | | 160°F | 250°F |
| STS-1 Configuration o Design Conditions (Model Test Loads) | 85 | 45 | -5 | 157 | 1.27 | 1.16 |
| o STS-1 Actual Impact Conditions (Model Test Loads) | 92 | 10 | -5 | 83 | 1.93 | 1.77 |

4. Aft Skirt Ring Capability. Since the loads predicted from model test data were not sufficient to cause the damage observed on the aft skirt rings, additional analyses were performed to define the failure modes of each ring. With skin pressures held constant and ring web pressures allowed to increase until failure occurs, the initial and sometimes secondary failure points were determined. The results of these analyses for the stiffening rings is given in Table 11. It can be seen that the analyses accurately predict the failure modes observed on STS-1, but the web pressure required to initiate failure is substantially greater than preflight predictions.

TABLE 11 AFT SKIRT RING CAPABILITY AT FAILURE PRESSURE

| | Failure Pressure* (psi) |
|--|-------------------------|
| Upper Ring Inner Flange Failure | |
| Ring Loads Only | 390 |
| Ring and Skin Loads | 335 |
| Aft Ring Failure | |
| Initial Failure of Lower Outboard Flange | 280 |
| Second Failure Would be Shear of Fasteners Between Gusset and Skin Stiffener | 400-450 |

*Factor of Safety = 1.0

5. Attrition Predictions. An analysis was performed [13] to define new attrition predictions based on STS-1 observations, i.e., early failure of the aft skirt thermal curtain and increased water impact loads on the aft skirt rings and the actuator attachment structure. The revised attrition estimates are compared to the preflight predictions in Table 12 for the actual STS-1 impact conditions. In general, the analyses show that an early failure of the thermal curtain has much less effect on attrition than does the estimated increase in water impact loads. In either case, the attrition rates are much higher than acceptable levels except for the actuator attachment structure.

TABLE 12. SRB ATTRITION ANALYSIS RESULTS

| | Attritions (%) (Databook Loads/ Est. New Loads) Yearly Nominal |
|---|---|
| Heat Shield Intact at Water Impact | |
| Aft Ring | 31.2/60.6 |
| Intermediate Ring | 44.9/87.8 |
| Forward Ring | 0.3/48.4 |
| Cascading (Actuator Attach System) | 6.12 |
| Heat Shield Failed Near 290 sec of Flight | |
| Aft Ring | 42.6/67.4 |
| Intermediate Ring | 55.6/92.8 |
| Forward Ring | 0.7/62.7 |
| Cascading (Actuator Attach System) | 6.72 |

- Note: 1. The attritions shown represent ultimate conditions.
 2. The numbers separated by a / are the attritions using the load data book reference compared to the load shown in Memorandum EP43(81-30).

C. Hardware Examinations

Post flight laboratory examination of SRB hardware was undertaken in several instances to help pinpoint the nature of observed anomalies and to define the specific damage incurred where this could not be determined visually.

1. Soot Composition. The black soot prevalent on the interior surfaces of the aft skirt was examined [14] for traces of aluminum (SRM propellant) and magnesium and silicon (SRM asbestos liner). No traces of aluminum oxide were found in the soot or contamination on painted surfaces. Significant quantities of magnesium and silicon were detected on all samples collected. While these could be indicative of asbestos, the ratio of magnesium to silicon was not relatively constant nor suggestive of asbestos. It was concluded that the source of the magnesium and silicon were more likely to have resulted from random dirt or seawater exposure.

2. TVC Component Fractures. Five failed A08 TVC hydrazine system components, consisting of overflow, purge, bypass, and feedlines, were examined visually and by fractographic and metallographic analyses [15]. From the visual and low power magnification examinations, extraneous molten teflon was discovered on the stainless steel tubing, and molten teflon was present on flex hoses. The line failures were all concluded to be caused by internal pressure which produced a ductile overload rupture. Microstructure and microhardness evaluations of the metallic components were both acceptable.

3. Aft Skirt Ring Material Properties. Tensile test specimens were taken from both the aft and intermediate rings on the A07 aft skirt [16,17]. The resulting data is given in Tables 13 and 14 for the aft ring and intermediate ring, respectively. In general, the properties were found to be above

TABLE 13. TENSILE TEST RESULTS SRB A07 AFT SKIRT LOWER RING SEGMENT

| Specimen Number | UTS (ksi) | TYS (ksi) | % e (1/2 in.) |
|-----------------|-----------|-----------|---------------|
| L-1 | 62,830 | 49,390 | 8 |
| L-2 | 65,470 | 51,170 | 7 |
| L-3 | 67,420 | 52,800 | 8 |
| L-4 | 68,990 | 54,510 | 8 |
| S-1 | 64,020 | 51,330 | 4 |
| S-2 | 63,320 | 49,800 | 4 |
| S-3 | 63,800 | 50,850 | 4 |
| S-4 | 60,110 | 51,170 | 4 |
| QQ-A-250/30 (T) | 57,000 | 42,000 | 4 |

NOTES:

1. L = Longitudinal; S = Short Transverse; T = Long Transverse.
2. QQ-A-250/30 = Long transverse only at 1/4 plate thickness.

TABLE 14. TENSILE TEST RESULTS FROM STS-1 AFT SKIRT INTERMEDIATE RINGS

| Specimen Number | UTS (ksi) | TYS (ksi) | % Elong. in 1 in. (4D) | |
|-----------------|------------------|-----------|------------------------|----|
| A07 | L-1 | 65,600 | 52,460 | 10 |
| | L-2 | 63,860 | 52,780 | 10 |
| | L-3 | 63,080 | 51,560 | 10 |
| | LT-1 | 64,580 | 52,600 | 6 |
| | LT-2 | 64,330 | 52,570 | 4 |
| | LT-3 | 61,260 | 50,460 | 6 |
| | ST-1 | 59,770 | 52,770 | 4 |
| | ST-2 | 57,610 | 52,670 | 3 |
| | ST-3 | 58,710 | 52,770 | 2 |
| A08 | L-1 | 64,010 | 53,180 | 6 |
| | L-2 | 63,870 | 52,750 | 6 |
| | L-3 | 63,640 | 52,330 | 6 |
| | LT-1 | 65,530 | 53,160 | 6 |
| | LT-2 | 63,700 | 52,820 | 6 |
| | ST-1 | 55,930 | 52,350 | 2 |
| | ST-2 | 56,200 | 52,470 | 1 |
| | ST-3 | 56,040 | 52,640 | 1 |
| | QQ-A-250/30 Req. | 61,000 | 49,000 | 3 |

NOTE: 1. QQ-A-250/30 requirements are for LT direction at 1/4 in. plate thickness.

the minimum specification allowable for both the longitudinal and long transverse directions. For the intermediate ring, however, the short transverse properties were found to be below the QQ-A-250/30 specification minimum ultimate tensile strength values (stated for long transverse direction only).

4. Failure Analyses of Rings. Visual, spectrographic, radiographic, metallographic, and fractographic analyses were performed on portions of the fractured ring segments for both the aft and intermediate rings of the A07 SRB [16,17].

a. Aft Ring. Failure analyses showed the failed segment to have sustained a ductile fracture with the fracture originating on the aft face of the web at its juncture with the outboard (skin) flange. The aluminum alloy material was within the acceptable limits of the purchasing specification, and there was no evidence of any unusual segregation of constituents or unusual grain size. Some corrosion, attributed to seawater exposure, was evident.

b. Intermediate Ring. The intermediate ring was determined to have sustained two ductile fractures of the outboard (skin) flanges. The two fractures were near and parallel to the ring web and progressed in opposite directions (Fig. 24). As with the aft ring, the aluminum alloy material exhibited no unusual segregation of constituents or unusual grain size. Spectrographic analyses of the ring were conducted on material from both near the center and near the surface, and the ring material was within the aluminum association chemical composition limits for 2024-T3 aluminum alloy.

5. Failure Analysis of Nozzle Actuator Brackets. As described earlier in this report, actuator brackets on the nozzle end of both A07 actuators failed during water impact loading. The failure analyses of these brackets [18] concluded that the brackets failed in a ductile manner as a result of a tensile overload. The fracture surface characteristics were found to be indicative of high velocity impact loads. The fracture modes of both brackets were determined to be essentially mirror images of each other with fractures initiating at the base of one of the pair of longitudinal lugs directly below the large holes accommodating the actuator attachment pins. In summary, the failures appeared to be the result of actuator tension loads, i.e., loads pulling away from the nozzle, with the fractures initiating on the left side of the left lug of the left-hand bracket and the right side of the right lug of the right-hand bracket at their juncture with the flanges bolted to the compliance ring. Mechanical properties of the brackets, derived from tensile specimens taken from the failed brackets, indicated a considerable variation. Strengths of the 7075-T73 forged material was significantly greater near the quenched surfaces and decreased near the center of the forging by as much as 15 ksi in ultimate tensile strength. This was not considered unusual for forgings of this geometry (6 to 7 in. thick), but was significant in that the failures initiated near the minimum strength portion of the brackets.

6. Postflight Dimensional Check. Because of the relatively severe damage on the aft skirts, a comprehensive series of optical measurements were taken on critical dimensions. These postflight measurements were then compared to recorded preflight values, where available, or to allowable drawing tolerances where preflight values were not recorded. The measurements taken are shown in Figures 25, 26, and 27, and the results are given in Tables 15 and 16. In general, it was found that some dimensional changes had resulted from the water impact loads, but that these changes were small and would not prevent reuse of the skirts after replacement of the damaged ring segments.

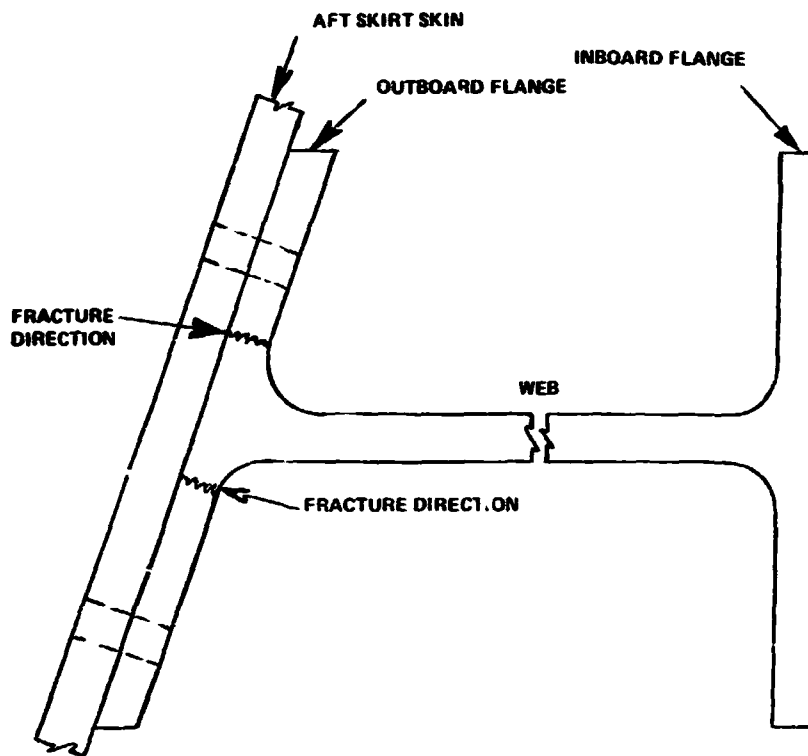


Figure 24. Aft skirt intermediate ring fracture directions (A07).

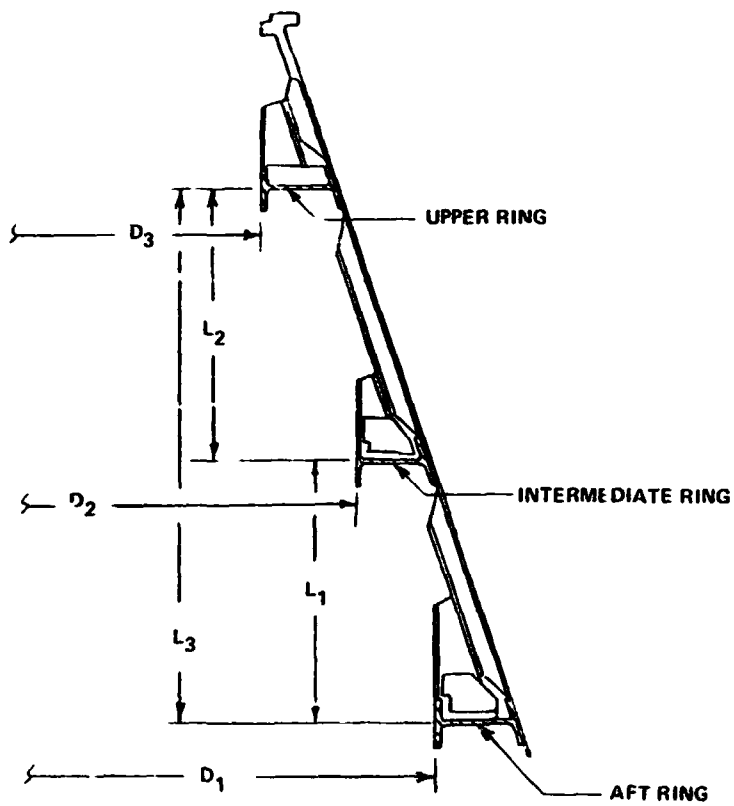


Figure 25. Aft skirt ring measurements.

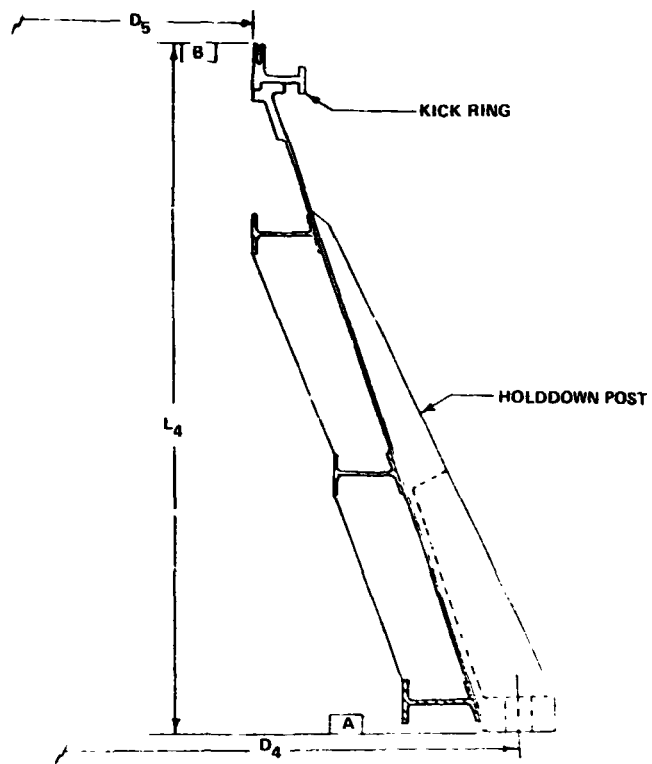


Figure 26. Aft skirt post and kick ring measurements.

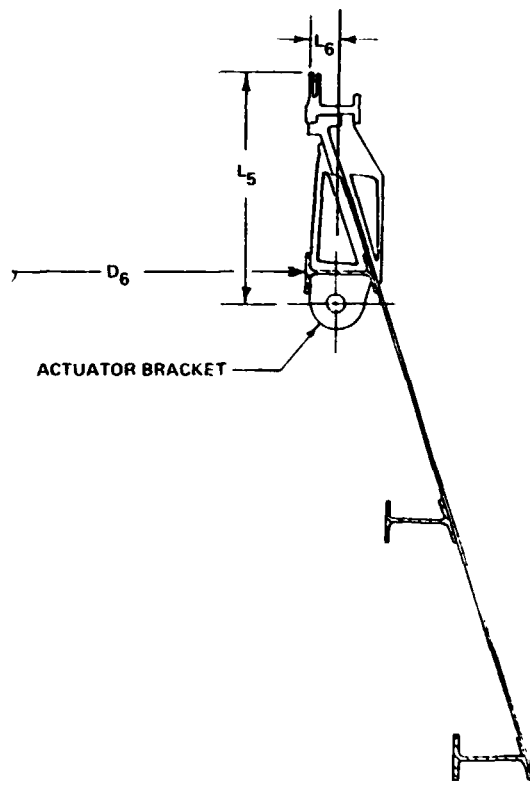


Figure 27. Aft skirt actuator bracket measurements.

TABLE 15. STS-1 AFT SKIRT POSTFLIGHT DIMENSIONAL CHECK RESULTS

| | Tolerance | A07 | A08 |
|--------------------------------------|--------------------|--------------------------------------|---|
| Bottom Plane of Aft Skirt | ±0.010 | In Plane | In Plane |
| Top Plane of Aft Skirt | ±0.010 | In Tolerance | In Tolerance |
| Aft Skirt Diameter at Holddown Posts | ±0.010 | In Tolerance | Out of Tolerance -0.032 & -0.100 in. |
| Actuator Bracket Location | | | |
| Axial | ±0.060 | In Tolerance | Out of Tolerance +0.025 & +0.047 in. |
| Radial | ±0.443 | In Tolerance | In Tolerance |
| Kick Ring Diameter | ±0.010 | Out of Tolerance -0.020 to -0.026 | Out of Tolerance -0.008 to -0.023 |
| Kick Ring Clevis Holes | -0.0005 +0.0025 | In Tolerance | In Tolerance |

TABLE 16. STS-1 AFT SKIRT POSTFLIGHT VERSUS PREFLIGHT DIMENSIONAL COMPARISON

| | Dimensional Change (Postflight - Preflight) | |
|---|--|------------------|
| | A07 (in.) | A08 (in.) |
| Aft Ring Diameter ¹ | -0.009 to +0.039 | -0.074 to -0.240 |
| Intermediate Ring Diameter ¹ | -0.014 to -0.048 | -0.011 to -0.040 |
| Upper Ring Diameter ² | -0.052 to +0.011 | -0.038 to +0.007 |
| Upper to Intermediate Ring Spacing ³ | -0.022 to +0.003 | +0.009 to +0.068 |
| Intermediate to Aft Ring Spacing ³ | -0.008 to +0.035 | Targets Lost |

1. Measured on Y-axis, Z-axis, and at holddown posts.
2. Measured on Y-axis, Z-axis, at holddown posts, and actuator locations.
3. Measured on Y-axis and Z-axis.

ORIGINAL PAGE IS
OF POOR QUALITY

FINDINGS

The ad hoc committee generated a number of findings using the data, inspections, analyses, and examinations which have been described earlier in this report. In general, these findings describe the most probable series of events leading to the damage incurred on the STS-1 hardware. These findings are given below with a brief discussion summarizing the pertinent evidence in support of each finding.

A. Finding 1

Failure of the SRB thermal curtain was precipitated, prior to reentry, by the initiation of the linear shaped charge (LSC) employed to jettison the SRM nozzle.²

Discussion. Thermal performance of the thermal curtain was nominal through the entire ascent heating regime (i.e., until after SRM burnout at 167 sec), but was almost totally lacking upon the earliest encounter with reentry aerodynamic heating. Two thermal curtain retainers at each SRM compliance ring interface were forceably detached prior to reentry smudging of the aft skirt interior surfaces [19]. The nozzle LSC is quite close to the thermal curtain retainers (Fig. 28), and problems with containing the blast without thermal curtain damage were experienced during static qualification firings of the SRM. The temperature rise recorded in the aft skirt cavity agrees quite well with preflight analyses for an assumed total loss of the thermal curtain at reentry [8].

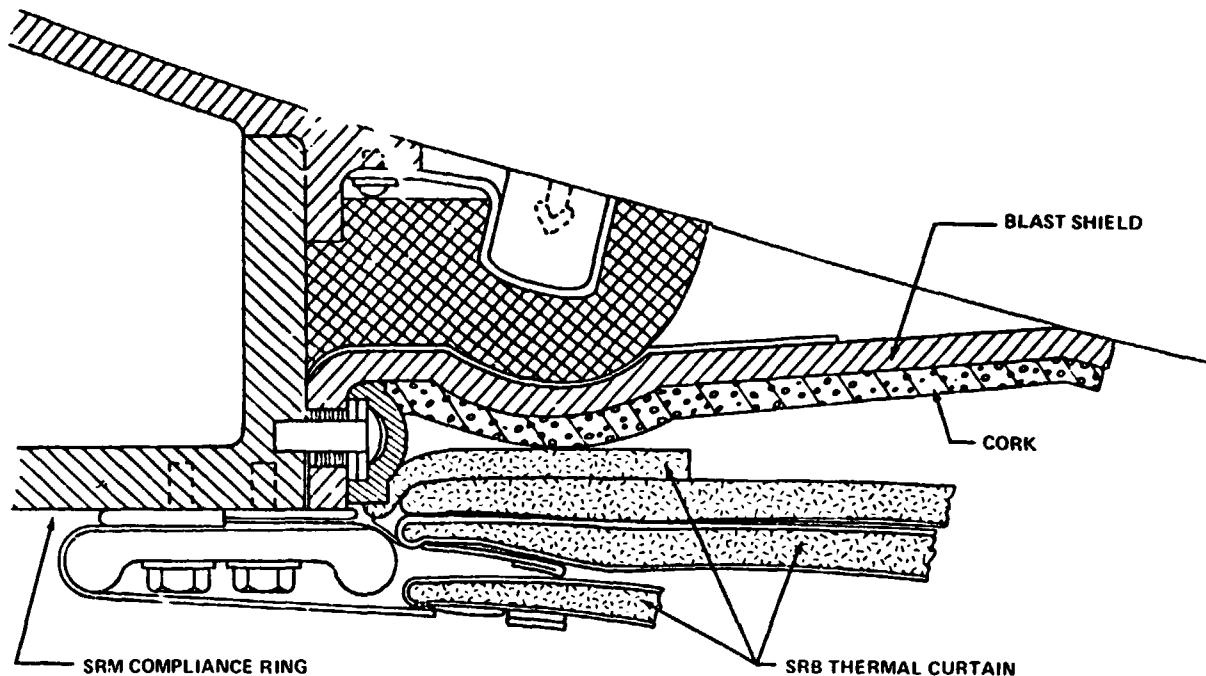


Figure 28. Nozzle LSC in relation to thermal curtain retainers.

2. Results of the STS-2 flight, where the nozzle LSC initiation was delayed until after parachute deployment, indicate that the thermal curtain will fail from aerodynamic phenomena (e.g., flutter) alone. Notwithstanding this, the evidence from STS-1 is conclusive that thermal curtain damage resulted from the early nozzle LSC initiation.

Finding 2

Aerodynamic heating was the principle cause of rupture of the TVC fuel system on A08 and the cable damage on both boosters.

Discussion. A postflight analysis of selected components which had suffered thermal damage showed that the temperatures necessary to cause the observed damage could be attained from aerodynamic heating alone [20]. The reentry burning, as seen on the movie coverage, is typical of that seen on ground static firings prior to CO₂ quenching, and generates only 3 to 5.5 Btu/ft² sec [9], much less than the 11 Btu/ft² sec reentry aerodynamic heating. Laboratory examination of the failed A08 TVC fuel lines indicates internal rupture of the tubing and ignition of the hydrazine after rupture. Although not conclusive, it is likely that the greater thermal damage observed on A08 is the result of hydrazine combustion after rupture of the fuel lines.

C. Finding 3

The SRM "afterburning" observed on both boosters during reentry was caused by burning of pyrolytic gasses from nozzle ablatives ignited by molten slag (Al₂O₃).

Discussion. The smoke color observed on the reentry films is black, which indicates burning of hydrocarbons rather than SRM solid propellant [14]. In addition, the smoke and fire are seen only after entry into the sensible atmosphere (about 16,000 ft) where the required oxygen is available to support combustion. SRM instrumentation recorded nozzle exit plane heating through nozzle jettison at 203 sec, and calorimeters went to zero at about 167 sec. A laboratory analysis of soot deposits on the aft skirt interior showed no traces of aluminum which would be present if SRM propellant were the fire's source. A Thiokol post-flight analysis showed that the ignition temperature required for pyrolytic gasses must be a minimum of 1470°F to 2080°F and the predicted slag (Al₂O₃) temperature would be 3200°F at the observed ignition time (368 sec) [9].

D. Finding 4

Cavity collapse loads were aggravated slightly by a reduced internal SRM pressure at splash-down resulting from higher-than-predicted internal case temperatures.

Discussion. The internal pressure of the SRM case during cavity collapse loading is largely dependent on the internal gas temperature immediately prior to water impact. A preflight analysis by Thiokol, which predicted a chamber gas temperature of 124°F, did not include effects of burning of pyrolytic gases during reentry. An updated, postflight analysis was performed by Thiokol [11] using worst case assumptions of complete combustion of both nozzle and chamber off-gases for the longest possible time (110 sec). This analysis showed the maximum internal temperature to be 1756°F. An MSFC analysis, based on the pressure collapse data of Figures 24 and 25, showed the ullage gas temperatures to be 830°F for A07 and 500°F for A08 [12].

E. Finding 5

External cavity collapse loads experienced on STS-1 boosters agree well with preflight predictions with the exception of the location of the peak pressure.

Discussion. From the limited data available from instrumentation on the SRM case, peak cavity collapse pressures agree well with the magnitude predicted by the scale model drop tests. There was some adjustment in longitudinal distribution indicated, in that the "leading edge" of the pressure peak was about 5 ft forward of the predicted location. The damage incurred on the SRM case and stiffening rings can be attributed to the forward location of the peak cavity collapse pressure, the actual STS-1 impact conditions (which were near those giving maximum cavity collapse loads), and the higher-than-predicted negative pressure inside the motor.

F. Finding 6

Water impact loads on the STS-1 aft skirt stiffening rings were substantially higher than pre-flight predictions.

Discussion. Although the water impact conditions, specifically the vertical velocity of the boosters, was outside the design envelope, preflight design load tables [21] encompassed the actual parameters experienced by the STS-1 boosters. Post-flight stress analyses showed that, at the actual impact, conditions seen by both A07 and A08, the structural loading predicted by the loads tables would not cause structural failure. Laboratory tests of tensile specimens taken from the failed A07 rings [16, 17] showed the basic material properties to be within specification allowables except for the short transverse direction which was not specified. Since it was determined that the short transverse direction was the failure direction in some instances, the minimum test value was used in subsequent analyses. A review of the geometry of the drop model used in generating design loads showed the model stiffening rings did not represent the actual flight rings in that their (radial) depth was less and there was no inboard flange. Also, the rings were not instrumented on the drop test model to obtain ring web pressures, so loads provided for ring stress analyses used measured skin pressures in the vicinity of the rings.

G. Finding 7

The A07 actuator brackets acted as a weak link, or "fuse," and prevented damage to other SRB components.

Discussion. Preflight attrition analysis [22] concluded that failure of the actuator attachment structural components would cause cascading failure of other aft skirt/nozzle-mounted components. It was also determined to be cost effective for these structural components to fail first, thus protecting the actuators from damage [23]. This effect was demonstrated on STS-1 (A07). Cascading damage did occur to two intermediate ring segments (and possibly an aft ring segment) and the aft exit cone shell from the bracket failures on A07. However, the actuators were undamaged and passed acceptance test requirements in postflight tests. Damage to the nozzle exit cone resulting from the bracket failures is repairable, as judged by Thiokol, but at a cost approaching 80 percent of new exit cone [24].

RECOMMENDATIONS

Based on the findings described in the previous section, the ad hoc committee formulated a number of recommendations leading to resolution of the problems encountered on the STS-1 flight. These recommendations deal principally with keeping the thermal curtain intact through the aerodynamic heating regime, if possible, and with redefining the water impact loads on the aft skirt stiffening rings.

**ORIGINAL PAGE IS
OF POOR QUALITY**

A. Recommendation 1

Delay SRM nozzle severance until after the main parachutes are deployed.

Discussion. Since the principal cause of early thermal curtain loss has been determined to be damage incurred at initiation of the nozzle LSC near apogee on STS-1, the delay of nozzle severance until main parachutes are deployed would effectively remove the source of the damage. Studies performed early in the SRB design stages had showed the late LSC initiation time to be feasible; however, reentry acoustics were thought to be higher than acceptable based on initial wind tunnel tests. Later wind tunnel tests have now shown the acoustic levels to be within acceptable limits. Another study performed as part of the ad hoc committee's activities shows that SRB reentry aerodynamic stability characteristics are generally more favorable, but that higher drogue parachute loads can result if the nozzle extension remains on during reentry. Higher internal SRM chamber gas temperatures are also possible because of an increase in exposed surface area of nozzle ablatives [11] and a larger "air scoop" to feed oxygen to any burning of pyrolysis gases. In the above cases, however, the risk of drogue parachute overload or sinkage of the SRB, respectively, have been carefully examined and found to be acceptable. Recontact of the SRB aft skirt with the nozzle extension in the water has also been studied and found to pose no undue risk.

B. Recommendation 2

Increase the strength of fasteners at the retainers for the thermal curtain at the SRM nozzle compliance ring.

Discussion. The two retainers immediately adjacent to the initiation point of the SRM nozzle LSC were detached on each of the STS-1 boosters. Evidence is conclusive that the retainer fasteners failed as a result of a tensile load induced by products of the LSC initiation blast [19]. Investigation has shown that the current 1/4-in.-diameter fasteners can be changed to 5/16-in.-diameter without impact to the design. This would provide nearly 60 percent increase in tensile strength and still permit increasing the fastener size to 3/8-in.-diameter if rework became necessary.

C. Recommendation 3

Improve development flight instrumentation to define water impact loads on aft skirt attachment rings.

Discussion. Only a limited number (4) of pressure transducers were available to provide water impact pressure data on STS-1 boosters, and these were confined to one booster [7]. The severity of damage to the structure obviously dictates that the design loads be redefined. First priority would appear to be adding active pressure transducers to all the ring webs. Perhaps an acceptable alternative would be the addition of many passive pressure sensors, in the form of burst discs, which would define, within limits, the peak pressures experienced throughout the aft skirt cavity. Precautions should be taken to ensure that active pressure sensors return data; i.e., thermal protection of the sensors and sensor wiring should be added in the event high heating is still encountered on future flights.

D. Recommendation 4

Perform additional SRB model drop tests to define aft skirt water impact pressures at design condition extremes.

Discussion. Design loads must be redefined to permit effective modification, or redesign, of the existing ring structures to preclude continued incidence of severe damage. While DFI, on early STS flight hardware, can provide valuable data on actual pressures encountered during water impact, it is unlikely that extremes of required design conditions will be seen during DDT&E flights. In particular, high horizontal velocities caused by wind conditions in the impact zone are unlikely because of DDT&E wind restrictions imposed at the launch site. Model drop data will provide the necessary data and can be correlated to similar conditions experienced on the full scale boosters.

E. Recommendation 5

Modify the design of the aft skirt stiffening rings to preclude high incidence of ring damage at water impact.

Discussion. Attrition analyses performed in light of the STS-1 damage indicate that aft skirt ring damage is highly likely on all future flights unless the ring structures are modified. Design studies and stress analyses have identified a number of structural modifications which will significantly improve the load-carrying capability of the rings. These proposed modifications include adding additional reinforcing gussets forward of all rings, adding brackets on the aft surface of the rings to support the inboard ring flange, adding an additional row of fasteners through the outboard (skin) flange of the rings, removing the aft skirt skin that projects aft of the aft ring flange, and adding brackets between the aft surface of the aft ring web and the aft outboard skin flange. In future ring buys, flange and web thicknesses could be increased.

F. Recommendation 6

Determine design mechanical properties in the short transverse direction for the plate stock from which the aft skirt stiffening rings are fabricated.

Discussion. The procurement specification for the thick plates used to fabricate aft skirt ring segments does not require minimum mechanical properties in the short transverse direction. Tensile test specimens made from STS-1 ring segments show the mechanical properties in the short transverse direction can be significantly lower than the longitudinal or long transverse properties [16]. Stress analyses of the rings and observation of STS-1 ring fractures show that some critical failure modes originate in the short transverse direction. Enough tensile tests need to be performed to establish a statistical data base for defining the minimum design values for the rings.

G. Recommendation 7

Evaluate the cost effectiveness of increasing the strength capability of the nozzle actuator bracket assembly at the SRM nozzle interface while retaining the weak-link concept (fuse) demonstrated on STS-1.

Discussion. The failure of the A07 actuator brackets on STS-1 appears to have prevented more serious (i.e., more costly) failures of the actuators and the structure adjacent to either end of the actuators. The successful postflight acceptance tests of the actuator and the reparable condition of such major structural members as the nozzle compliance ring and nozzle shell indicate the actuator brackets perform effectively as a "fuse" when excessive nozzle loads are encountered. However, an increased capability of the brackets could lessen the frequency of bracket failure and still retain the desired feature of protecting the actuators [22].

H. Recommendation 8

Evaluate the need for adding stiffening rings to the stubs on the SRM forward stiffener case segment.

Discussion. Cavity collapse loading on STS-1 was determined to peak about 5 ft further forward than predicted by model drop tests. Coupled with the greater pressure drop now predicted in the SRM chamber at splashdown, the differential pressure in the aft SRM segments will be greater than that used for design. The forward stiffener case segment on the A07 booster (s/n 019) sustained damage primarily because of the forward shift of the peak water pressure. The cavity collapse loading experienced on STS-1 boosters was near the maximum value ever to be expected in future flights. Since the preliminary assessment of the recovered segments indicates the forward stiffener segment can be reused, it may not be cost effective to add the two stiffeners.

REFERENCES

1. Brisson, E. H.: Quality Observations of SRB-A08. United Space Boosters, Inc., letter EHB-051-81-MQA, May 1981.
2. Souther, C. H.: SRB STS-1 Aft Skirt Cable Damage. NASA letter EC42 (49-81), May 1981.
3. Souther, C. H.: SRB STS-1 Aft Skirt Cable Damage. NASA letter EC42 (51-81), June 1981.
4. Hein, L. A. and Hughes, R. W.: SRB STS-1 Damage Investigation Committee Damage Assessment, TVC. NASA letter EP33 (81-34), May 1981.
5. Anonymous: SRM Project Quarterly Review. Thiokol/Wasatch Division, August 1981.
6. Stein, S. R.: Space Shuttle STS-1 Structural Assessment of Stiffener Ring Performance from Post-Flight Inspection at KSC. Thiokol/Wasatch Division Report TWR-13051, July 1981.
7. Anonymous: Space Shuttle STS-1 Final Flight Evaluation Report, Volume I. NASA/Marshall Space Flight Center, July 1981.
8. Sterett, J. B.: SRB Aft Skirt Structure Thermal Response for STS-1. NASA letter EP44 (81-61), July 1981.
9. Eckhardt, K. R.: Progress Report on STS-1 Reignition During Reentry Investigation. Thiokol/Wasatch Division Inter-Office Memo 2815-81-M043-1002, June 1981.
10. Sterett, J. B.: Thrust Vector Control (TVC) Hydraulic, Fuel and Electrical Line Thermal Response to STS-1 Reentry Heating Environment. NASA letter EP44 (81-53), June 1981.
11. Eckhardt, K. R. and Hopen, D. P.: Thermal Analysis of STS-2 Nozzle LSC During Reentry for Unsevered Exit Cone. Thiokol/Wasatch Division Inter-Office Memo 2815-81-M050-1002, June 1981.
12. Sterett, J. B.: STS-1 Solid Rocket Booster (SRB) Flotation Evaluation. NASA letter EP43 (81-28), June 1981.
13. Thionnet, C. L.: STS-1 Damage Assessment. NASA letter EL44 (81-36), July 1981.
14. Riehl, W. A.: SRB Burning Phenomena on Reentry. NASA letter EH31 (81-31), June 1981.
15. Gilmore, H. L.: STS-1, SRB-A08, TVC Hydrazine Tubing Components (Rock and Tilt) (M and FA W/O 81-023). NASA letter EH22 (81-91), September 1981.
16. Hess, J. H.: Metallurgical Analysis of Failed SRB Aft Skirt Intermediate Ring (STS-1, A07). NASA letter EH23 (81-104), October 1981.
17. Hess, J. H.: Metallurgical Analysis of Failed SRB Aft Skirt Lower Ring (STS-1, A07). NASA letter EH23 (81-94), September 1981.

REFERENCES (Concluded)

18. Hess, J. H.: Mechanical Property Evaluation and Failure Analysis of SRM Nozzle Actuator Brackets from STS-1. NASA letter EH23 (81-80), July 1981.
19. Thionnet, C. L.: Thermal Curtain Failure Investigation. NASA letter EL44 (81-35), July 1981.
20. Sterett, J. B.: STS-1 Hydrazine Leak Thermal Environment Assessment. NASA letter EP44 (81-56), June 1981.
21. Anonymous: SRB Loads Data Book. NASA Report SE-019-057-2H, December 1975.
22. Hopson, G. D.: Evaluation and Failure Assessment of the STS-1 SRM Nozzle Actuator Bracket and Exit Cone Shell. NASA letter EL01 (292-81), October 1981.
23. Cornelius, C. S.: STS-1 SRB TVC Actuator Post-Flight Assessment. NASA letter EC21 (158-81), July 1981.
24. Dorsey, E. G.: Damaged STS-1 Nozzle Aft Exit Cone Shell. Thiokol/Wasatch Division letter 7000/ED-81-360, September 1981.

APPROVAL

**SPACE SHUTTLE STS-1 SRB DAMAGE INVESTIGATION
FINAL REPORT**

By Clyde D. Nevins

The information in this report has been reviewed for technical content. Review of any information concerning Department of Defense or nuclear energy activities or programs has been made by the MSFC Security Classification Officer. This report, in its entirety, has been determined to be unclassified.


J. A. McCool
Director

Structures and Propulsion Laboratory